Spring 2008

Integrated process planning for a hybrid manufacturing system

Lan Ren

Department: Mechanical and Aerospace Engineering

INTEGRATED PROCESS PLANNING FOR A HYBRID MANUFACTURING SYSTEM

by

LAN REN

A DISSERTATION

Presented to the Faculty of the Graduate School of the

MISSOURI UNIVERSITY OF SCIENCE AND TECHNOLOGY

In Partial Fulfillment of the Requirements for the Degree

DOCTOR OF PHILOSOPHY

in

MECHANICAL ENGINEERING

2008

F. W. Liou, Advisor	D. A. McAdams
K. Chandrashekhara	X. Du
J. W. Newkirk	

PUBLICATION DISSERTATION OPTION

This dissertation consists of the following three papers that have been accepted or submitted as follows:

Pages 3-34 have been accepted in the Proceedings of MSEC2007 International Manufacturing Science and Engineering Conference.

Pages 35-63 have been accepted in the proceedings of the ASME 2007 International Design Engineering Technical Conferences& Computers and Information in Engineering Conference and submitted for publication to ASME Transaction, Journal of Computing and Information Science in Engineering.

Pages 64-102 have been submitted for publication to the SME Journal of Manufacturing Processes.

ABSTRACT

A hybrid manufacturing system integrates CNC machining and laser-aided layered deposition and achieves the benefits of both processes. In this dissertation, an integrated process planning framework which aims to automate the hybrid manufacturing process is investigated. Critical components of the process planning, including 3D spatial decomposition of the CAD model, improvement of the toolpath generation pattern, repairing strategies using a hybrid manufacturing system, etc., are discussed. 3D part decomposition based on modular boundary models and centroidal axis extraction methods are combined to decompose parts more robustly and reliably. Coverage toolpath planning focuses on the toolpath coverage efficiency and the strategies to predict the possibility of the occurrence of deposition voids so that the appropriate toolpath pattern can be applied to avoid deposition voids. The contour-parallel offsetting pattern and the adaptive zigzag toolpath pattern are applied as the alternate options and the final adaptive deposition coverage toolpath will be the combination of these two basic patterns depending on the prediction results of the occurrence of the deposition voids. As an extended application of a hybrid manufacturing system, part repairing strategies have been developed utilizing the hybrid manufacturing system due to the benefits of cost reduction as well as time and energy savings. The hybrid manufacturing system and the process planning software elevate the repairing and manufacturing process to the next level, in which accuracy, reliability, and efficiency can be achieved. Experiments are implemented to validate the feasibility and reliability of the integrated process planning strategies.

ACKNOWLEDGMENTS

I would like to give my thanks to two groups of people who have contributed much to me during my doctoral program – those who helped me in my academic development, and those who helped me in my personal life.

First of all, I want to express my sincere gratitude to my advisor, Dr. Frank Liou, for providing guidance and constant encouragement during my PhD program. He provided a good working environment and supported me in every aspect beyond my research. I also want to express my appreciation to group members' discussions and suggestions, especially Mr. Todd Sparks and Dr. Jianzhong Ruan. Appreciation is extended to my advisory committee members for their valuable time, efforts and review of this dissertation. In particular, Dr. K. Chandrashekhara introduced me to the Finite Element Analysis; Dr. McAdams, Dr. Du and Dr. Newkirk gave me many useful suggestions during the preparation of this dissertation. Financial support from NSF DMI-9871185, U.S. Air Force Research Laboratory contract # FA8650-04-C-5704, Intelligent System Center, and Department of Mechanical and Aerospace Engineering are gratefully acknowledged.

Finally, I want to express my deep appreciation to my husband, Gang Duan, brother, Chao Ren, especially my parents, Yuancun Ren and Rongju Chen, for their endless encouragement, patience, and support.

TABLE OF CONTENTS

Page

LIST OF ILLUSTRATIONS

LIST OF TABLES

INTRODUCTION

A multi-axis hybrid manufacturing system includes a Layered Manufacturing unit and five-axis CNC machining center together, and the resulting hybrid process can provide greater building capability, better accuracy and surface finish by achieving the benefits of both processes. This system has been developed in the Laser-Aided Manufacturing Processes (LAMP) Laboratory in the University of Missouri-Rolla (UMR). An integrated process planning software is developed to facilitate the users for the hybrid manufacturing system in order to build functional metal parts automatically. The purpose of the process planning software is to build the functional parts by combining deposition and machining using the hybrid manufacturing system in the LAMP lab in an automatic mode within one setup and without much human interference. The software is programmed using HOOPS as the display engine and ACIS as the modeling kernel and has been developed using Visual C++ programming language. The CAD model in this dissertation is in .SAT format, which is the surface boundary representation of a solid model.

This dissertation focuses on the following topics. (i) Process planning for 3D metal deposition without support structures is investigated. 3D part decomposition based on modular boundary models and centroidal axis extraction methods are combined to decompose the CAD model of a to-be-manufactured part into some sub-components more reliably. The multi-axis slices will be generated for every component to avoid the need for a support structure. (ii) An improved adaptive deposition toolpath pattern is developed for the multi-axis slices to generate the deposition coverage path. Different from the existent toolpath generation patterns, this improved pattern will handle the

deposition void problem by detecting the possibility of the occurrence of a deposition void and then automatically choosing the appropriate toolpath pattern. Because a single toolpath pattern is either inefficient enough or possibly causes the deposition void, this adaptive toolpath pattern will ensure complete coverage of the target geometry with consideration of the time efficiency of deposition process by combining multiple toolpath patterns. (iii) Process planning for five-axis surface machining is implemented to improve the manufacturing quality after the deposition is finished. Then the process planning for five-axis CNC machining and Laser-Aided Deposition will be integrated and interfaced onto the same software framework platform to complete the process planning for the hybrid manufacturing system. Based on the integration, the whole process of 3D part manufacturing can be finished in a totally automatic mode without human interference after one initial setup. (iv) Part repairing strategies will be investigated as an extended application of the hybrid manufacturing system and also as validation of the integrated process planning. The strategies will include feature replacement and surface-patching methods. Feature replacement consists of defining the damaged features by user assistance, machining out the defined feature, and then depositing the damaged features. Surface patching is designed especially for repairing the damaged surfaces by depositing layers of materials on the damaged face and then finish machining the repaired surfaces. It is another extended application of the hybrid manufacturing system.

PAPER I

PART REPAIRING USING A HYBRID MANUFACTURING SYSTEM

Lan Ren[1], Kunnayut Eiamsa-ard[2], Jianzhong Ruan[1] and Frank Liou[1]

[1]Department of Mechanical and Aerospace Engineering, University of Missouri-Rolla, Rolla, MO 65409-0050

[2]Department of Mechanical Engineering, Kasetsart University, Bangkok, 10900 Thailand

ABSTRACT

At present, part remanufacturing technology is gaining more interest from the military and industries due to the benefits of cost reduction as well as time and energy savings. This paper presents the research on one main component of part remanufacturing technology, which is part repairing. Traditionally, part repairing is done in the repair department using welding processes. However, the limitations of the traditional welding process are becoming more and more noticeable when accuracy and reliability are required. Part repairing strategies have been developed utilizing a hybrid manufacturing system in which the laser-aided deposition and CNC cutting processes are integrated. Part repairing software is developed in order to facilitate the users. The system and the software elevate the repairing process to the next level, in which accuracy, reliability, and efficiency can be achieved. The concept of the repairing process is presented in this paper, and verification and experimental results are also discussed.

1. INTRODUCTION

Part repair technologies have been employed in many military and industrial applications such as torpedo shells, dies, molds, and turbine blades repair. Damage can occur during the operations or handlings. As shown in Figure 1, defects or damages can be categorized into four main types: crack, worn-out surface, corroded surface, and broken parts [1].

The size of the damage is used to classify each type of damage. The damage is classified as a crack if the width is tiny but the depth and the length of the damage are relatively large. Heat stress induces cracks in dies or molds and cracks in ship steel are caused by fatigue. If the width and length of the damage are large compared with the depth, then the damage is defined as a worn-out surface. Worn-out surfaces are typically seen in parts with movements such as shafts. Corroded surfaces usually occur on parts in extreme environments, such as inserts of molds and torpedo shells.

Common processes used in the part repair process are Gas Tungsten Arc Welding (GTAW) and Tungsten Inert Gag (TIG) welding. These traditional repair processes contain five basic steps [2]: (a) The damaged part is cleaned and the defects are identified, and then grease and other impurities are removed; (b) The damaged part is then pre-heated; (c) Filler is added via the welding process; (d) After welding, the part is then set aside to rest to relieve it from expansion due to the heat; and (e) Finally post-heat is applied to relieve the stress. However, there are some limitations of the welding process in part repair. The welding process cannot achieve high accuracy and reliability, and the deformation of the repaired part is usually large. Also the bonding between the filler and

the damaged part is always poor. More importantly, some of the metal materials are not weldable.

To solve some of these problems, a cold repair process called Metalock process has been used, which avoids the stress due to the heat. Holes are drilled along the cracks and then tapped and filled with studs. The repaired pieces are not fused to a single piece. This method requires highly skilled technicians.

Laser welding process is another method that has been used in part repair. Laser welding process possesses advantages over the conventional welding process. For example, the heat-affected zone is relatively small compared with the welding processes. Thus, the deformation and stress are relatively small. Laser welding process can also be used with virtually any kind of material including unweldable materials. The time required for repairing is significantly reduced, and accuracy and repeatability can be achieved. However, this process limits itself to repairing cracks only due to the nature of the process.

The following section summarizes the applications of the part repair processes. In a work done by Camp and Bergan [3], torpedo parts were repaired using the laser-aided repair process. Motor shafts [4-5] and ship steel [6] were repaired using laser-aided repair processes. The corroded and worn-out dies and molds were fixed in the work done by Roy and Francoeur [7] as well as in the work done by Skzek and Lowney [8]. Laser welding was used to repair the corroded steam generator tubes in nuclear plants [9], and turbine blades were repaired using the laser cladding process [10-11]. The work done by Wang et al. criticized that the process planning for these repair processes is application specific [2].

2. REPAIR STRATEGIES

In this paper, the hybrid manufacturing system combines Layered Manufacturing and CNC machining. The resulting hybrid process can provide a greater build capability and better accuracy and surface finish by achieving the benefits of both processes [12-14]. Layered Manufacturing method used in this paper is Direct Metal Deposition (DMD) process, which utilizes a high-powered laser to melt metal powder layer-by-layer on the substrate to directly manufacture fully dense metal parts. Aiming at the main categories of defects shown in Figure 1, two repairing strategies using different toolpath generation patterns were advanced, which will be called feature replacement and surface patching later in the paper. As the name shows, feature replacement means the method of machining the damaged feature out and depositing back the repaired feature and it is designed especially for repairing cracks and broken parts. In contrast, surface patching is only applicable for another two categories of defects: corroded or worn-out surfaces. These two strategies will be demonstrated in detail later. Meanwhile, the repair process planning software is developed to facilitate users on the VISUAL C++ programming platform, using ACIS as the modeling kernel and HOOPS as the graphics display engine.

2.1. Feature Replacement Method

In this strategy, the damaged feature is machined off and deposited back, and then surface machining brings the whole repairing process to the end. The process planning procedures are as follows: a) define the to-be-repaired feature, b) generate the contour offsetting machining toolpath to machine out the damaged feature, c) generate the contour offsetting depositing toolpath to deposit back the feature to the original, and d)

post-process the toolpath data to get the CNC codes file for a specified hybrid manufacturing system. The contour offsetting has been studied extensively. Many approaches exist for constructing the offset paths for the 2-D contours. These methods can be categorized into three groups: pair-wise offset [15], pixel-based [16], and Voronoi approaches [13, 17-22]. Some of the earlier works reported that their algorithms can be successfully used with arbitrary shapes [15-16, 20-21]. In general, the offset curves can be defined using Minkowski operations described below.

2.2. Minkowski Operations (Sum and Subtraction)

Minkowski operations have been used in the areas of image processing and robotics path planning. Minkowski Sum and Minkowski Subtraction are known as dilation and erosion, respectively, in the area of image processing. Let A and B be sets as shown in Figure 2. $A \oplus B$, the Minkowski Sum of set A and set B, denotes the sum or the addition of the two sets. Minkowski Sum is defined as follows:

$$A \oplus B = \{a + b : a \in A \text{ and } b \in B\} \tag{1}$$

It is common to write A+b instead of $\{a + b: a \in A\}$. Thus, $A \oplus B$ can also be defined as follows:

$$A \oplus B = \bigcup \{A + b : b \in B\} = \bigcup_{b \in B} \{A + b\} \tag{2}$$

Similarly, the Minkowski Subtraction ($A \ominus B$) is defined as fllows:

$$A \ominus B = \bigcap \{A + b : b \in B\} = \bigcap_{b \in B} \{A + b\} \tag{3}$$

2.3. Interior, Closure, and Boundary Operations

Let X be a closed set (i.e. X = {x: x∈X}). The interior of set X is the union of all open sets within X, denoted as int(X). Note that int(X) is necessarily an open set. The closure of set X, denoted as cl(X), is the intersection of all closed sets containing X, and cl(X) must be closed. The boundary of set X, denoted as ∂(X), is its closure minus its interior.

$$\partial(X) = cl(X) - \text{int}(X) \tag{4}$$

2.4. Offset Paths

Let R be the target region in which the coverage paths are planned, and let T be the virtual tool shown as a planar disk in Figure 3. Also, at iteration i, let O_i be a set in which the distance from the contour to any points in the set is larger or equal to a fixed distance, di (di = i * D, where D = diameter of the tool or laser diameter - overlap). The boundary of set R as ∂(R) is the contour boundary of the target region.

At iteration i, the set O_i is equivalent to Minkowski Subtraction of the set O_{i-1} and the tool area (T). The deposition path $\partial(O_i)$ is defined as:

$$\partial(O_i) = \partial(O_{i-1} \Theta T) = \partial(\bigcap_{t \in T} O_{i-1} + t) \tag{5}$$

2.5. Path Generation

The following is a repair example to illustrate how this strategy works. Figure 4 shows the damaged part before defining the damaged feature and after the damaged feature is removed.

The paths for deposition and surface finish machining were generated automatically using the contour offsetting pattern and zigzag pattern, respectively in the software developed with Visual C++. The results are shown in Figure 5. From the figure, the defined damaged feature was sliced, and the toolpath was generated for every slice. The toolpath were then sent to a postprocessor to generate the NC codes.

The drawback of the above repair strategy is that for worn-out or corroded surfaces, pre-machining is unnecessary. This implies that replacing the damaged feature is not the best strategy for finishing a repair job. Also, the contour offsetting toolpath pattern sometimes cannot guarantee the deposition quality because of the possibility of generating the porosity and bad surface evenness during deposition. Aiming at the above limitations, the surface patching method is investigated using the adaptive zigzag toolpath pattern especially for the worn-out or corroded surfaces in this paper. For a worn-out surface, the materials can be deposited on the damaged surface directly using the adaptive zigzag toolpath without pre-machining. The major difference between those two toolpath generation patterns will be demonstrated in detail in the later sections.

2.6. Surface Patching Method

Surface patching method is a process planning strategy especially for repairing worn-out and corroded surfaces by a hybrid manufacturing system. It uses the adaptive zigzag toolpath pattern for toolpath generation, which changes the raster direction in the connective layers compared with the traditional zigzag machining toolpath [23-24]. Figure 6 shows the difference among the contour offsetting pattern, the traditional zigzag toolpath pattern along a fixed direction, and the adaptive zigzag toolpath pattern for

deposition along interlaced directions. As the figure demonstrates, the major difference between those two zigzag patterns is the travel direction. Instead of a fixed direction in Figure 6(b), the travel direction in Figure 6(c) keeps switching in every connective layer, e.g., the horizontal direction in the first layer, the vertical direction in the second layer, and then the horizontal direction in the third layer again and so on. The other difference is that the boundary of the surface needs to be traveled first in the adaptive zigzag pattern, and then the offsetting surface area (the offsetting distance is usually the size of the laser spot) is filled by an interlaced zigzag toolpath. The reason why the boundary of the original surface needs to be traveled first and then offset to get the target area for filling the toolpath is because the extra materials will not be deposited on the boundary and the boundary will not be over-deposited as to destroy the surface evenness. Apparently, this will reduce the chances of the occurrence of porosity. As far as the traveling direction is concerned, usually the two principle axes of the target area are considered to be the best choices.

Figure 7 demonstrates the adaptive zigzag toolpath generated by the process planning software for the connective two layers of the triangular target area. The distance between these two layers is the layer thickness depending on the different operation parameters in the hybrid manufacturing system. As shown, the target area is created by offsetting the original triangular surface. The toolpath for the bottom layer (Layer I) travels along the horizontal direction, while the traveling direction for the top layer (Layer II) is vertical with the previous travel direction (horizontal direction).

Figure 8 shows two deposition results of the same geometries obtained from two different toolpath patterns. In (a), the target geometry is filled by the contour offsetting

pattern, and in (b) the toolpath pattern is the adaptive zigzag pattern discussed above. As shown in the figure, the surface evenness of (b) is much better than the surface evenness of (a). Also, Figure 8(a) shows that there is a hump in the middle of the target area, which often happens when depositing by the contour offsetting pattern.

Another advantage of this toolpath pattern is its feasibility and generality for a curved surface, which means it can follow the surface contour and act like the meshing grid of the curved surface. From another point of view, the adaptive zigzag toolpath can even be considered as the parametric curve expressions along two major axes that completely retain the surface contour information. Figure 9 shows the adaptive surface patching zigzag toolpath for the curved face in both 2-D and 3-D modes generated by the repairing process planning software.

It can be seen that 2-D surface patch zigzag toolpath is generated by filling the projected area of the target face on an X-Y plane, and it actually loses most information about the target curved surface. Being different from the 2-D surface patch, the 3-D surface patch keeps almost all the feature information of the target surface and definitely will result in a better deposition quality in most situations. Whether to use the 3-D surface patch actually depends on the curvature of the curved surface. Experimental results prove that the deposition quality almost stays the same when using either a 2-D or 3-D surface patch if the curvature is not very high. However, for high curvature, deposition using the 2-D surface path is even unsuccessful and the 3-D surface patch undoubtedly is the optimal strategy.

2.7. Toolpath Generation for Complicated Geometry

Concerning toolpath generation methods, one more issue was studied in this paper, which is the toolpath generation strategy for complicated geometries. For certain complicated shapes that include at least one inner loop or concave vertex, in order to avoid crossing the loops, the geometry must be divided into several sub-regions, among which any one has no inner loops or a concave vertex. Then every sub-region will become the target area, and the same toolpath generation method is used as discussed above to obtain reasonable toolpath separately. Here the cell decomposition algorithm is adapted to divide the target area into different sub-regions which are then filled by a certain toolpath pattern [25-26]. In Figure 10, the adaptive zigzag toolpath pattern is used to fill every sub-region as an example. After the target area is broken into sub-regions, the certain toolpath generation algorithm is used for every sub-region, and the boundary for every sub-region needs to be traveled before filling it with the zigzag toolpath to guarantee the features of the inner loops. Finally, the total toolpath for the complicated geometry divided into some sub-components is the summation of the toolpath for every single sub-region. Concerning the connection toolpath among all the sub-regions, the rapid travel lines are applied to realize the transition from one sub-region to the next.

3. EXPERIMENTS

The repairing strategies discussed above have been applied on the mold/die repair for Spartan Light Metal LLC. Figure 11 shows the damaged die core before repairing and after deposition by the surface patching strategy after the damage was identified as worn-out surfaces. The top portion of the die is damaged and all the surrounding worn-out

surfaces need to be repaired. Here the surface patching pattern was used to generate the adaptive zigzag toolpath to finish repairing all the surrounding damaged surfaces in an automatic mode without human interference. The whole repair job was finished in one setup, and the reliability of the repair job was greatly improved. The laser used was a NUVONYX 1K max diode laser. The laser processing parameters for cladding steel H13 powder were 600W with a stand-off distance from the nozzle to the top of the clad of 0.5 inch. The powder feed rate for H13 powder was 6g/min. The NC code was set to move the nozzle up 0.02 inch after each layer which is the layer thickness mentioned before. The travel speed of the nozzle was 20 inches/minute, and the track width was 0.05 inch.

Figure 12 shows three moments of repairing three different damaged surfaces, respectively. The whole repair job took less than 10 minutes except for the time for setting up the part. This proves that the surfacing patching method is much more effective compared with the feature replacing method for repairing corroded or worn-out surfaces. The surface patching method is an effective strategy to repair the usual kinds of damages in the die industry with high reliability.

4. DISCUSSIONS

4.1. Bonding Strength

The interfacial strength is determined from a four-point bend test, as shown in Figure 13. The four-point flexture test is based on the storage of a known amount of elastic energy on bending and a release of this elastic energy on fracture. Interfacial cracks propagate when the strain energy release rate equals to the critical energy release

rate (Gc) of the interfacial failure. Four-point bend test has been used to analyze the interface between the substrate and the cladding produced by laser processing.

Ashcroft et al. calculated the critical energy release rate (interfacial energy) for thick claddings [27]. Several critical parameters have been added into the calculation such as the thickness of the substrate, width of the substrate, and the thickness of the cladding itself as shown below.

$$G_c = (18 \bullet E_f \bullet d \bullet F_c^{\,2} \bullet l^2 / b^2 \bullet T^6 \bullet E_s^2)(T^2 + d^2/3) \quad (6)$$

where

E_f = Modulus of elasticity of the cladding;

d = Thickness of the cladding;

F_c = Critical load corresponding to de-lamination;

l = Distance between the inner and outer rollers;

b = Width of the substrate;

T = Thickness of the substrate; and

E_s = Modulus of elasticity of the substrate.

The 50 x 6 x 1 mm specimens are cut out from the deposition. A center pre-crack is made on the specimen in order to induce symmetrical cracks along the clad-substrate interface. The specimen is then loaded in a four-point flexture on an Instron TT-B Universal Testing machine until a new crack propagates through the entire cladding. The interfacial fracture energy of the laser cladding tool steel specimen is compared to the tool steel weld specimen of the exact same dimensions. The test data in Table 1 shows the comparison between the welding samples and the deposition samples. The calculation

results for interfacial fracture energy show that the bonding strength of the repaired part done in hybrid manufacturing systems is better than that of the welding process.

4.2. Thermal Conductivity

Another important mechanical property for mold/die repair is the thermal conductivity. In metals, a relationship exists between thermal and electrical conductivity. This relationship, known as the Wiedemann-Franz Law, states the ratio of thermal conductivity to electrical conductivity is proportional to the metal's temperature.

$$k / \sigma = LT \tag{7}$$

where

k = thermal conductivity

σ = electrical conductivity

L = Lorenz numbers

T = temperature

This property can be exploited to make thermal conductivity measurements by making electrical resistance measurements. Fairly accurate results can be achieved for simple geometries where the resistivity can be computed from the resistance, while more qualitative measurements can be made for more complex parts. (i.e. The test could tell if part A had better conductivity than part B.) The test results in Figure 14 show that the deposition repair has the best thermal conductivity. Furthermore, the most practical evaluation is to test the repaired part in the real engineering environment. The above repaired die has been tested by Spartan Light Metal LLC and the result is very satisfying.

5. CONCLUSIONS

This study shows that parts with different types of defects can be repaired in hybrid manufacturing systems by using either the feature replacement method or surface patching method. Accuracy and reliability can be achieved with the integration of the hardware and software automatically without human intervention. The bond strength and the thermal conductivity of the repaired part done in hybrid manufacturing systems are better than those of the welding process. Thus, hybrid manufacturing systems have the potential to repair damaged parts. For the complicated geometry divided into sub-components, the deposition sequence among all the sub-components is another research issue. In this paper, the transition among all the components is traveled rapidly. The optimized sequence will definitely enhance the deposition quality.

ACKNOWLEDGEMENTS

This research was supported by the National Science Foundation Grant Number DMI-9871185, the grant from the U.S. Air Force Research Laboratory contract # FA8650-04-C-5704, and UMR Intelligent Systems Center. Their support is greatly appreciated.

REFERENCES

1. Wang, J., Prakash, S., Joshi, Y., and Liou, F., Laser aided part repair - a review, Proceedings of the Thirteenth Annual Solid Freeform Fabrication Symposium, Austin, TX, August 5-7, 2002.
2. Sammons, M., Learning the art of tool and die welding repair, Die Casting Engineers, 43(5), 1999.
3. Camp, J.D., and Bergan, P., Implementation of laser repair process for Navy aluminium components, Diminishing Manufacturing Sources and Material Shortages Conference, August 21 – 24, 2000.
4. Wang, J., and Zhuang, T., Motor shaft repairing by laser cladding, Laser Processing of Materials and Industrial applications, November, 1996.
5. Vuorista, P., Laser coating as an industrial coating process, Ceramics Coatings and Surface Treatments Conference, September 10-11, 2002, Tampere, FINLAND.
6. Brown, P.M., Shannon, G., Deans, W., and Bird, J., Laser weld repair of fatigue cracks in ship steels, Welding Research Abroad, 1999:45(12), 7-13.
7. Roy, S., and Francoeur, M., Options for restoring molds, http://www.joiningtech.com/pdfs/moldrestoration.pdf, accessed July 2005.
8. Skzek, T.W., and Lowney, M.T.J., Die reconfiguration and restoration using laser-based deposition, Solid Freeform Fabrication Proceedings, 2000, 219-226.
9. Wowczuk, A., Miller, R., and Bruck, G., Robotic laser welding system improves steam generator repair, Power Engineering, 1990.
10. Sexton, L., Lavin, S., Byrne, G., and Kennedy, A., Laser cladding of aerospace materials, Journal of Materials Processing Technology, 2002:122, 63-68.

11. Richter, K., Orban, S., and Nowotny, S., Laser cladding of the titanium alloy TI6242 to restore damaged blades, Proceedings of the 23rd International Congress on Applications of Lasers and Electro-Optics, 2004.
12. Frank Liou, Jianzhong Ruan, A Hybrid Metal Deposition and Removal System for Rapid Manufacturing, International conference -- 2002 April: San Antonio, Metal powder deposition for rapid manufacturing.
13. Ruan, J., Eiamsa-ard, K., and Liou, F.W., Automatic process planning of a multi-axis hybrid manufacturing system, Journal of Manufacturing System. (in print)
14. F. W. Liou, J. Choi, R. G. Landers, V. Janardhan, S. N. Balakrishnan, S. Agarwal, Research and Development of a Hybrid Rapid Manufacturing process, Solid Freeform Fabrication Symposium, Austin, TX, 2001.
15. Choi, B.K., and Park, S.C., A pair-wise offset algorithm for 2D point sequence curve, Computer –Aided Design. 1999:31(12):735-745.
16. Choi, B.K., and Kim, B.H., Die-cavity pocketing via cutting simulation, Computer Aided Design 1997:29(12):837-846.
17. Ruan, J., Eiamsa-ard, K., Zhang, J., and Liou, F.W., Automatic process planning of a multi-axis hybrid manufacturing system, Proceedings of DETC'02, September 29 – October 2, 2002, Montreal, CANADA.
18. Held, M., On the computational geometry of pocket machining, Springer-Verlag, Berlin, Heidelberg, 1991.
19. Held, M., Lukas, G., and Andor, L., Pocket machining based on contour parallel tool path generation by means of proximity maps, Computer Aided Design 1994:189-203.

20. Eiamsa-ard, K., Liou, F.W., Landers, R.G., and Choset, H., Toward automatic process planning of a multi-axis hybrid laser aided manufacturing system: skeleton-based offset edge generation, Proceedings of DETC'03, September 2 – 6, 2003, Chicago, IL.
21. Kao, J., and Prinz, F.B., Optimal motion planning for deposition in layered manufacturing, Proceedings of DETC'98, September 13 - 16, 1998, Atlanta, GA.
22. Kao, J., Process planning for additive/subtractive solid freeform fabrication using medial axis transform, Ph.D. Thesis, 1999, Stanford University, CA.
23. Misra, D., Sundararajan, V., Wright, P. K., Zig-Zag Tool Path Generation for Sculptured Surface Finishing, Dimacs Series in Discrete Mathematics and Theoretical Computer Science, 2005, VOL 67, 265-280.
24. Zhiyang Yao, Satyandra K. Gupta, Cutter path generation for 2.5D milling by combining multiple different cutter path patterns, International Journal of Production Research, June 2004, Vol. 42, No. 11, 2141-2161.
25. Choset, Howie, Coverage of Known Spaces: The Boustrophedon Cellular Decomposition, Autonomous Robots 9, no. 3 (2000): 247-253.
26. Acar, Ercan U, Choset, Howie, Rizzi, Alfred A, Atkar, Prasad N, Hull, Douglas, Morse, Decompositions for Coverage Tasks, The International Journal of Robotics Research 21, no. 4 (2002): 331-344.
27. Ashcroft, I.A., and Derby, B., Adhesion testing of glass-ceramic thick films on metal substrates, Journal of Materials Science, 1993:28(11), 2989-2998.

Table 1. Interfacial energy (J/m2) comparison between deposition and welding on die/mold repair case.

Properties	Notation	Laser cladding (Best Parameter from Experiments)	Weld
Modulus of Elasticity of Cladding (Pa)	Ef	2.10E+011	2.10E+011
Thickness of cladding (meter)	d	2.00E-003	2.00E-003
Critical load of delamination (N)	Fc	11428	11438
Distance between inner and outer rollers (m)	l	1.00E-002	1.00E-002
Width of Substrate (m)	b	6.00E-003	6.00E-003
Thickness of substrate (m)	T	8.00E-003	8.00E-003
Modulus of Elasticity of Substrate (Pa)	Es	2.10E+011	2.10E+011
Interfacial fracture Energy or Bond Strength (J/m^2)		15499.44	15526.58
Difference		27.14	

(a) (b)

Figure 1 Types of damages: (a) Crack (b) Worn-out or corroded surface.

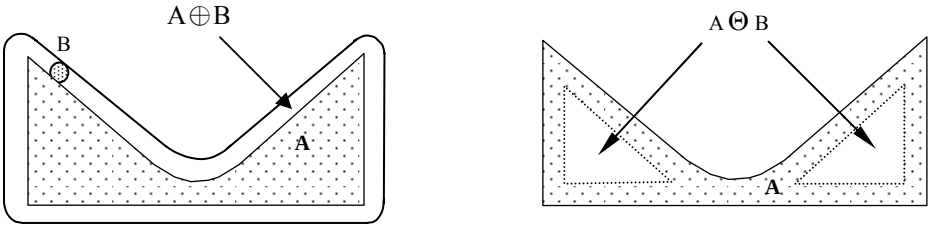

Figure 2 (a) Minkowski sum $A \oplus B$ and (b) Minkowski subtraction $A \ominus B$.

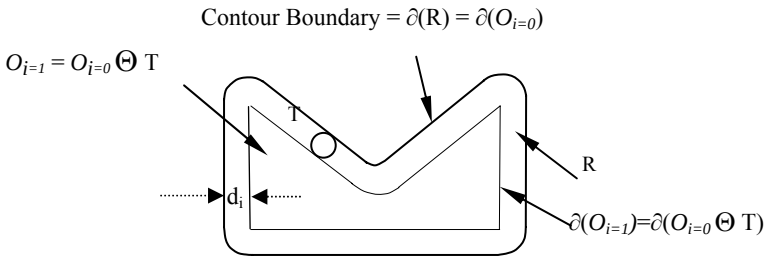

Figure 3 Relationship between the offset curve and Minkowski subtraction ($O_{i=0} \Theta T$).

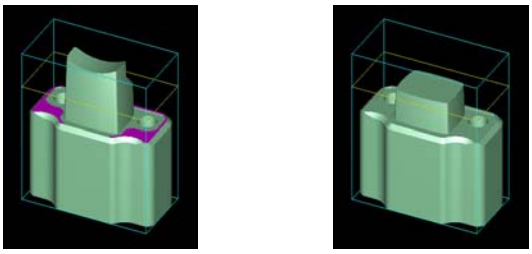

(a) (b)

Figure 4 (a) The entire cutting plane option and (b) the part after removing the damaged feature.

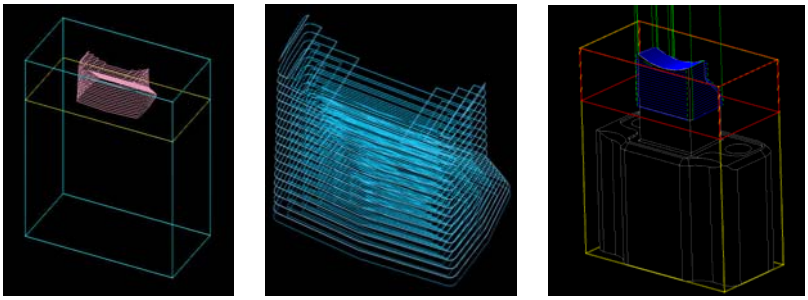

(a) (b) (c)

Figure 5 (a) Slices and (b) Deposition paths (close up) (c) Surface machining toolpath.

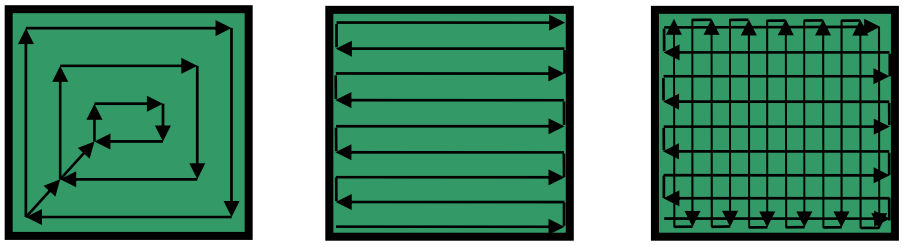

(a) (b) (c)

Figure 6 Different toolpath generation patterns (a) Contour offsetting (b) Zigzag (fixed direction) (c) Zigzag (interlaced direction).

.

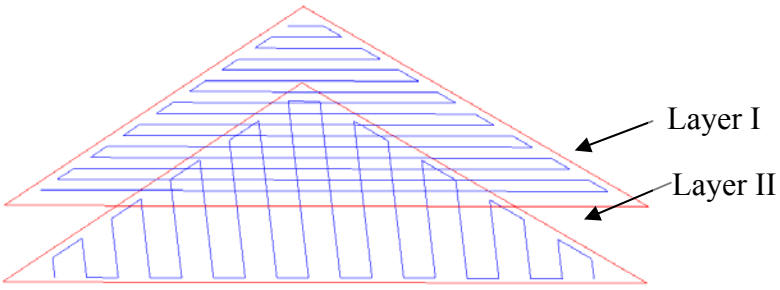

Figure 7 Interlaced zigzag toolpath in two connective layers.

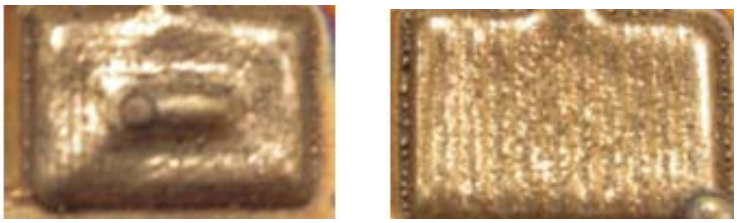

Figure 8 Depositions obtained from two different toolpath patterns.

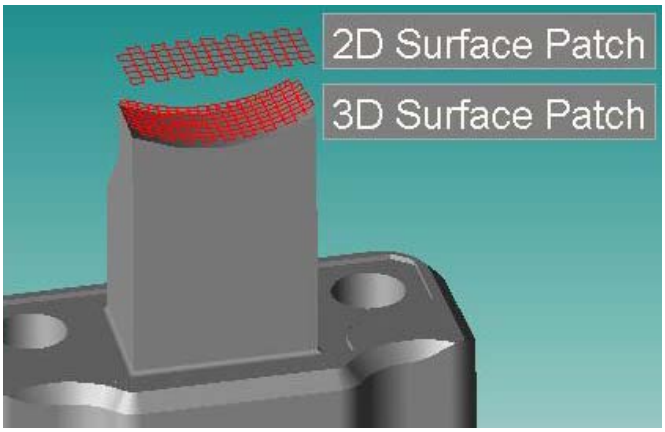

Figure 9 Surface patching zigzag toolpath for a curved surface.

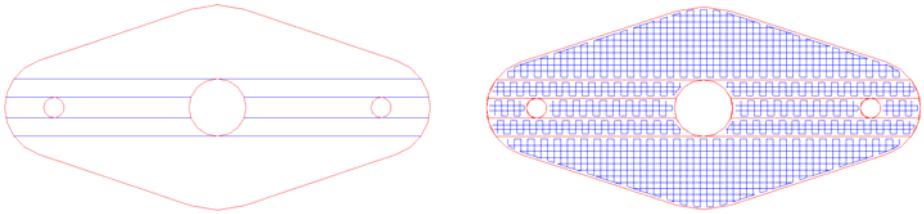

Figure 10 Complicated geometry filled by the interlaced zigzag toolpath.

(a) (b) (c)

Figure 11 Die core repaired via surface patching (a) Before repairing (b) After deposition (c) After surface machining.

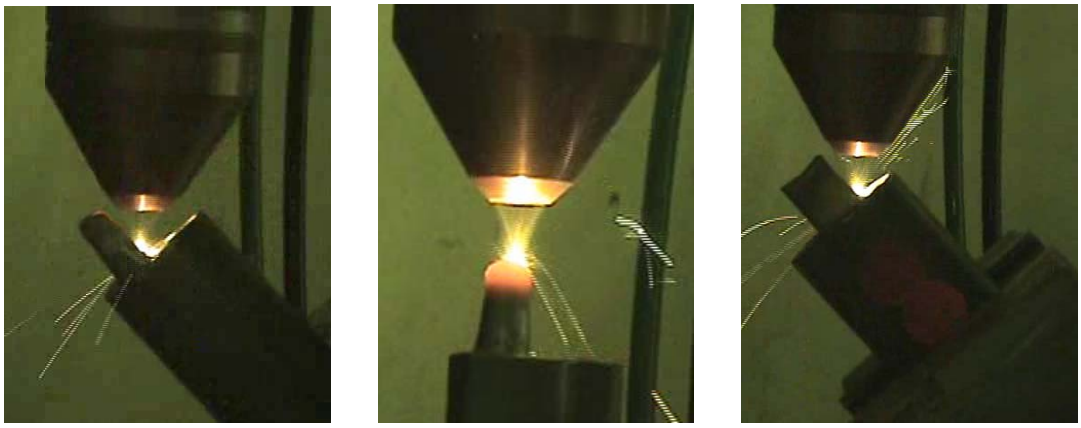

Figure 12 Automatic repairing processes.

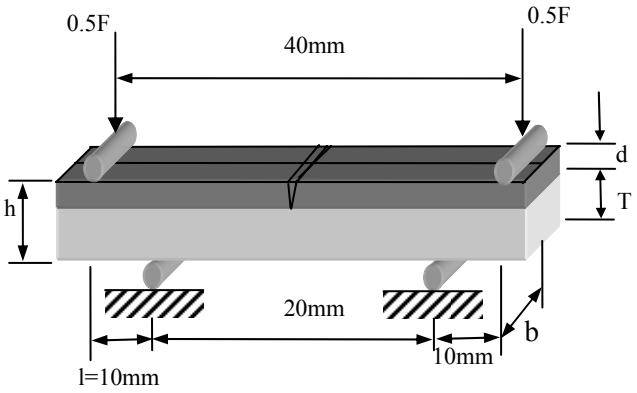

Figure 13 Bending test setup.

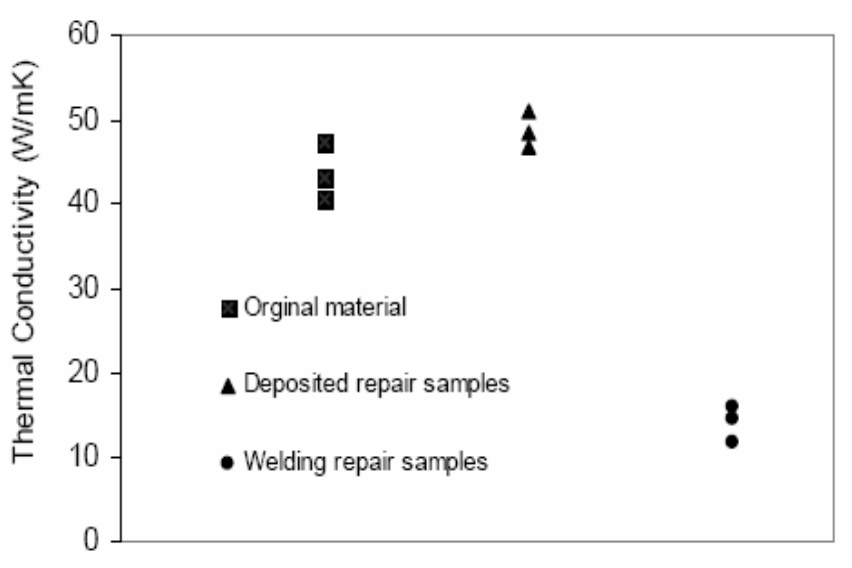

Figure 14 Thermal conductivity comparisons.

PAPER II

ADAPTIVE DEPOSITION COVERAGE TOOLPATH PLANNING FOR METAL DEPOSITION PROCESS

Lan Ren[1], Kunnayut Eiamsa-ard[2], Jianzhong Ruan[1] and Frank Liou[1]

[1] Department of Mechanical and Aerospace Engineering, University of Missouri-Rolla, Rolla, MO 65409-0050

[2] Department of Mechanical Engineering, Kasetsart University, Bangkok, 10900 Thailand

ABSTRACT

Coverage toolpath planning is very critical to deposition quality in layered manufacturing especially for metal deposition processes. The correct choice of toolpath patterns will make it possible to build a fully dense and functional metal part. The major consideration when selecting a toolpath pattern is the complete coverage of the to-be-deposited geometry which means no voids should happen. This paper presents the research on the toolpath coverage efficiency and the strategies to predict the possibility of the occurrence of deposition voids so that the appropriate toolpath pattern can be applied to avoid deposition voids. The contour-parallel offsetting pattern and the adaptive zigzag toolpath pattern will be applied as the alternate options and the final adaptive deposition coverage toolpath will be the combination of these two basic patterns depending on the prediction results of the occurrence of the deposition voids. The experiment has demonstrated that the adaptive toolpath pattern can greatly improve the reliability of the coverage path planning in deposition processes.

1. INTRODUCTION

The coverage toolpath in both machining and deposition has been studied extensively as an important component of process planning [1-4]. Although many researchers did studies on the optimization of the toolpath planning strategies [5-7], the major toolpath generation patterns in the current research work are still as follows: contour offsetting pattern [8-10] and zigzag pattern. The contour offsetting pattern includes the contour-parallel offsetting pattern and spiral offsetting pattern. For toolpath planning for machining including the complicated freeform surface machining, the zigzag toolpath generation pattern is still the most prevalent pattern because of its simplicity and efficiency [11]. For rapid manufacturing industry, the contour-parallel offsetting pattern and spiral offsetting pattern are often adopted due to the nature of additive manufacturing technology. Besides those patterns mentioned above, some research about combining the existent toolpath patterns to generate hybrid toolpath has been performed also. Even though the deposition void problem which is called the undercut region if it happens in toolpath planning for machining is still a research issue. Some methods have been advanced in order to achieve the complete coverage deposition toolpath generation.

In [12], the spiral offsetting toolpath was utilized in the deposition toolpath generation instead of the contour-parallel offsetting pattern. The spiral offsetting pattern can avoid the occurrence of the deposition void in some cases and achieve better coverage efficiency than the contour-parallel offsetting pattern. But in some situations where deposition void probably happens at more than one spot, the spiral offsetting toolpath cannot efficiently avoid the occurrences of all the possible voids. Figure 1 shows an example of deposition void using a spiral offsetting toolpath pattern after the top

surface was machined. In the close up view Figure 1 (b), the void can be observed very clearly. In this case, the deposition void happened at one of the four corners of the geometry. It can be considered as the uncut area in machining toolpath planning. Obviously, the spiral offsetting toolpath pattern can alleviate the possibility of the occurrence of deposition void. However, it cannot always cover the target area very well depending on the different geometries.

Like the uncut region in CNC machining, the deposition void problem is also a research issue of coverage toolpath planning for the deposition process. In order to avoid the occurrence of the deposition void, it is necessary to explain the reason why deposition void happens and to define the types of deposition void. Figure 2 lists the major types of void which often happened when depositing. Usually, a deposition system includes a laser generation cell and a powder feeding unit. The deposition process used in this paper is the Direct Metal Deposition (DMD) process which utilizes a high power laser to melt metal powder layer by layer on the substrate to manufacture fully dense metal parts directly [13-14]. Here the laser used was the NUVONYX 1K max diode laser which is located in the Laser Aided Manufacturing Process (LAMP) lab at University of Missouri–Rolla.

As Figure 2 shows, the grey area represents the area where certain types of void will happen. Three types of void often happened when using the contour-parallel offsetting pattern. Void type I happens if the area to be deposited needs to be covered with more materials but it is not big enough to hold one more offset loop because offsetting distance is too large. Void type II often happens when the corner of the geometry has a sharp angle which is smaller than a certain value depending on the

process parameters of the different rapid manufacturing systems. In that case, the void usually will happen at the corner which has a sharp angle. Void type III happens if the offsetting algorithm generates more than one loop. Apparently, a void will happen in the area between the separated two loops in this case.

In this paper, the adaptive deposition toolpath will be the research focus, aiming at predicting the occurrence of deposition void and adjusting the toolpath pattern automatically to avoid the occurrence of the deposition void. At the same time, efficiency is another objective which needs to be considered in the adaptive coverage toolpath strategy discussed in the following sections.

This paper is organized as follows: in the next section, the related work is summarized. The existent toolpath patterns are compared and the improved adaptive toolpath pattern is illustrated in Section 3. The experiments are performed and the results are discussed in Section 4. The paper is concluded in Section 5.

2. LITERATURE REVIEW

Some research has been done in order to resolve the deposition void problem which is also called gap in some papers. In the literature [12], the spiral offsetting pattern was adopted instead of contour-parallel offsetting pattern to avoid the occurrence of the deposition void at the sharp corners. The disadvantage of this strategy is that it cannot handle the cases where more than one sharp angle exists because of the nature of the spiral offsetting pattern. Figure 3 explains the reason why the spiral offsetting pattern has better coverage than the contour-parallel offsetting pattern. In Figure 3(a), it can be seen that there are three loops including the biggest loop which is the boundary of the target

area. It shows that there will be four spots marked by a red circle, respectively where deposition void probably happens if the contour-parallel offsetting pattern is used. In Figure 3(b), it shows that the possible deposition void at the right side of the triangular area was avoided because the spiral offsetting toolpath goes to the inner loops from those corners on the right. Because the geometry in Figure 3 has more than one sharp angle, the spiral offsetting toolpath cannot avoid the possible deposition void at all the corners. In all, the spiral offsetting pattern usually can avoid the deposition void when the deposition geometry only has one sharp angle for every inner loop in the toolpath.

Besides the spiral offsetting pattern, a combination of toolpath patterns is another method to solve the deposition void problem. In the research done by Yao and Gupta [15], multiple different cutter path patterns were combined for 2.5D milling to generate the improved cutter path which is significantly superior to the path generated by a single pattern. The objective of the above strategy is to find the most efficient toolpath which is the shortest path to cover the area to be machined. And the computational time needed may be a bottleneck. What's more, the machining toolpath is somehow different from the deposition toolpath although the uncut region in machining can be considered as the coverage void in deposition processes. One important difference is about the repetition of the same machining toolpath which causes cutting the "air" in some sense. But the repetition of the deposition toolpath will result in the over-deposition of extra materials which will finally destroy the surface evenness greatly. In [16], multiple combinations of the toolpath generation patterns have been studied in deposition processes, and a deposition cell was defined. The solution for the deposition void was achieved by adjusting the toolpath, i.e., adding some straight lines to cover the area where a void may

happen. This method can somehow fill the small void; however, some bigger void cannot be filled with just several straight lines, and the surface evenness will be impaired as well. So the method of filling the voids with several lines is not always effective. Another easy method is to decompose the target area into several loops and to use the different toolpath patterns in different loops.

In this paper, an adaptive toolpath generation pattern was advanced when coverage and efficiency are both considered as the objectives with the assumption that coverage has higher priority. The zigzag pattern [17-18] and contour offsetting pattern will be used as the candidates and the algorithm was developed to predict the possibility of the occurrence of deposition void and switch to the appropriate toolpath pattern automatically when needed. The alternation between these two patterns will be determined by the algorithm automatically whenever the possibility of the occurrence of the voids is detected. Meanwhile, the process planning software is developed to facilitate users on the VISUAL C++ programming platform, using ACIS as the modeling kernel which includes the functions for all basic methods for CAD modeling and HOOPS as the graphics display engine.

3. ADAPTIVE TOOLPATH STUDY

3.1. Zigzag and Spiral Offsetting Patterns

In this paper, the zigzag pattern and contour-parallel offsetting pattern will be the options we can choose from. We need to decide which one is more efficient so that it can be made as the first choice when there will not be void happened when using either one of those two patterns. It is worthy to note that the zigzag toolpath generation pattern in

this paper is slightly different from the traditional zigzag machining toolpath. Figure 4 shows the difference between the traditional zigzag toolpath pattern along a fixed direction and the adaptive zigzag toolpath pattern for deposition along interlaced directions discussed in this paper. As Figure 4 demonstrates, the major difference between those two zigzag patterns is the traveling direction. Instead of a fixed direction in Figure 4(a), the traveling direction in Figure 4(b) keeps switching in every connective layer, e.g., the horizontal direction in the first layer, the vertical direction in the second layer, and then the horizontal direction in the third layer again and so on. The other difference is that the boundary of the surface needs to be traveled firstly in the adaptive zigzag pattern, and then the offsetting surface area (the offsetting distance is usually the size of the laser spot) is filled by an interlaced zigzag toolpath pattern. The reason why the boundary of the original surface area needs to be traveled firstly and then offset to get the target area for filling the zigzag toolpath is because the extra materials will not be deposited on the boundary and the boundary will not be over-deposited. As far as the traveling direction is concerned, usually the two principle axes of the target area are considered to be the best choices.

Figure 5 shows the same to-be-deposited area filled by the toolpath generated from the contour-parallel offsetting pattern and adaptive zigzag pattern, respectively. From Figure 5, it also can be seen that the traveling direction of the zigzag pattern here is alternated for every connective layer.

After the traveling direction is switched back, two layers of materials will be deposited on the substrate. In Table 1, the toolpath length compared is with regard to two layers of deposition. Deposition time is only dependent on toolpath length generated by

the different toolpath generation patterns because all the other process parameters are same including the traveling speed and the time for setup etc. By computing the path length listed in Table 1, we can see the contour-parallel offsetting toolpath pattern is more efficient than the adaptive zigzag pattern as far as the deposition time is concerned. But it also can cause the deposition void because of the nature of the contour-parallel offsetting algorithm discussed above. The contour offsetting toolpath will be used as the default deposition path generation pattern. And it will be replaced by the zigzag pattern only when the deposition void is predicted because of better coverage efficiency of the adaptive zigzag pattern. The algorithm for detecting the possibility of occurrence of the deposition void will be discussed in the next section in detail.

After the contour-parallel offsetting pattern is defined as the default pattern because of its efficiency, the prediction algorithm for deposition void needs to be developed which will be illustrated in the following section. This algorithm will determine when the toolpath pattern should be switched by detecting the possibility of the occurrence of the deposition void.

3.2. Deposition Void Prediction

Figure 6 demonstrates how the deposition void happens in the real deposition process using an isosceles triangular shape as an example. Same as the fact that the machining toolpath is for the bottom center of the cutting tool, the deposition toolpath is for the bottom center of the laser nozzle. Here in this paper we have a laser whose spot size is *D* marked below, and the overlap is 50% which means the offsetting distance used for contour-parallel offsetting algorithm is *(1-ovelap)D=D/2*. As shown in the figure, we

pick a spot marked by a red ellipse in Figure 6 (b) as an observation spot to study the principle of the occurrence of deposition void. In Figure 6 (a), there are two connective paths which are denoted *Pn* and *Pn+1*. The blue and red patterns denote the covered area after the laser nozzle travels along *Pn* and *Pn+1*, respectively. Here only the area between *Pn* and *Pn+1* needs to be considered. The area which cannot be covered by the materials twice is defined as the area where the deposition void will possibly occur. And the deposition void area can be computed with the method discussed below. Another major function used in this paper is called AreaDif(). This function takes two arguments which are two regions and calculates the difference of area of those two arguments.

In Figure 7, it is assumed that C is the sweeping region of the laser spot shown by a circle along the inner toolpath loop B, and the face bounded by the outer loop A and inner loop B are denoted by S_A and S_B, respectively. The area bounded by the outer loop A and the inner loop B is the to-be-deposited target area. Based on the types of deposition void discussed before, area difference can be used as the major criteria to predict the occurrence of deposition void for generality. If the area difference calculated by function AreaDif() between S_A and the union of the sweeping region C and S_B is larger than or equal to the tolerance δ, then the adaptive zigzag pattern will be adopted. Otherwise, the contour-parallel offsetting pattern which is the default pattern is the option. Because of the coverage efficiency of different rapid manufacturing methods, the tolerance δ needs to be figured out specifically by designing some experiments using relevant experiment design methods, and it depends on the deposition process parameters in different rapid manufacturing systems, such as laser spot size, overlap, etc.

The program routine is like the following. Zigzag (G, P1, P2…) is the function for generating the adaptive zigzag toolpath for a given geometry. G denotes the given geometry and P1, P2 etc. denote the process parameters, e.g. laser power, track width, feed rate of the worktable etc. It is the same for the function Offset (G, P1, P2…) except that it is used to generate the contour-parallel offsetting path. The program will stop until the whole target area is covered by either one type of toolpath or a combination of both.

Set the contour of the target area as the current toolpath loop

Loop

If ($AreaDif(S_A,(C \cup S_B)) \geq \delta$)

{

Zigzag pattern is chosen;

Zigzag (G, P1, P2…);

}

Else

{

Contour offsetting pattern is chosen;

Offset (G, P1, P2…);

}

Set the generated new toolpath loop as the current loop

Loop End

Here, $C \cup S_B$ denotes the union operation of region C and S_B explained in Figure 7.

3.3. 2D Cell Decomposition

For certain complicated shapes which include inner loops or concave vertex, in order to avoid crossing the loops, the geometry needs to be divided into several sub-regions among which any one has no inner loops or concave vertex. Then every sub-region will become the target area and the same adaptive toolpath generation method is used to get reasonable complete coverage toolpath separately. Here cell decomposition algorithm [19-20] is adapted to divide the target area into different sub-regions which will then be filled with the adaptive zigzag toolpath pattern. Figure 8 is a flowchart which shows the major steps of the decomposition algorithm used in this paper. The input for this algorithm is any kind of 2D geometry and the list of the final decomposed striped cells will be returned. After the target area is broken into sub-regions, the adaptive toolpath generation algorithm will be used for every sub-region, and the boundary for every sub-region needs to be traveled before filling with the adaptive toolpath to guarantee the feature of the inner loops.

Figure 9 demonstrates an example of the 2D decomposition algorithm. The algorithm started by computing the principal axes of the original region which are X and Y axis in this case. X axis was selected as the scanning direction here, and the extreme positions on every inner loop along Y axis were found to construct a set of parallel planes which are vertical with the original region. The intersection results of this set of plane and the original region were a set of edges. This set of edges divided the original region into some striped regions. After cell decomposition, the original geometry was divided into seven striped sub-regions denoted as C1, C2, etc. Clearly, the decomposition algorithm used here will avoid the unnecessary deposition in order to guarantee the inner loops.

Figure 10 shows two examples to illustrate the adaptive toolpath planning by combining the contour-parallel offsetting pattern and the adaptive zigzag pattern. Different from the example shown in Figure 9, the regions here does not have any inner loops. However, the cell decomposition is still needed for better coverage because the region will be broken into more than one loop if contouring offsetting toolpath pattern is used for the whole region. For the geometry which only has one loop, the simplified decomposition is realized by scanning the region along two principle axes to find a set of broken lines. The position where the shortest broken line happens is usually the spot where the contour-parallel offsetting loops will be possibly broken into separate loops. And those shortest lines will be used as parting lines which are shown as CI in the figure. As Figure 10(a) shows, the dimension of the cross section of the part is 2.5 inch x 2.0 inch, and the first two loops of the toolpath for sub-regions are generated by the contour-parallel offsetting pattern since the contour-parallel toolpath pattern is the first choice if it won't cause the deposition void. After detecting the possibility of the occurrence of deposition voids, the toolpath generation pattern is switched to the adaptive zigzag pattern immediately to avoid the possible deposition void.

In Figure 10 (b), for the sub-region on the left, obviously contour-parallel offsetting is not applicable at all. So the sub-region on the left is filled by the adaptive zigzag toolpath pattern from the beginning. And it is obvious to observe that there is a sharp angle at one corner of the left sub-region. Obviously, the sharp angle is the major reason why the toolpath pattern switches to an adaptive zigzag pattern from the first loop. Also the figure shows that the 2D cell decomposition algorithm is used to divide the target area into several separated cells for complicated geometries especially when the

inner loops or concave vertex exist. Here, CI means cell interface between every two connective cells.

4. DISCUSSIONS

In the following experiment, the laser processing parameters for cladding steel H13 powder were 600W with a stand off distance from the nozzle to the top of the clad of 0.5 inch. The travel speed of the nozzle was 20 inches per minute. The powder feed rate for H13 powder was 8g/min. The track width used here is 0.1 inch with the overlap being 50%. The tolerance δ discussed above was defined as with the help of experiments by advance. For the deposition system in this paper, δ equals to 0.015 square inch after carrying out the designed experiments. Figure 11 demonstrates the deposition results using the adaptive toolpath pattern. The part has the same geometry as the one in Figure 10(a) and the dimension is 2.0 inch x 2.0 inch for cross section. After machining out the top surface, obviously no deposition void happened when using the adaptive toolpath shown in Figure 10 (a). The deposition result is very satisfying and the object of fully dense part building is achieved.

5. CONCLUSIONS

This paper presents the adaptive toolpath generation pattern aiming at resolving the deposition void problem in layered manufacturing efficiently. The advantage of this pattern over other existent toolpath patterns is its coverage efficiency with the consideration of the time efficiency at the same time. Also the algorithm can predict the possibility of the occurrence of the deposition void and choose the appropriate toolpath

pattern when needed automatically. By the experimental validations, it is approved that the adaptive toolpath pattern is more robust to deal with the deposition void problem than other patterns when the objective is both coverage efficiency and time efficiency and it can be used as an improved path planning strategy to build the fully dense and functional metal parts efficiently.

ACKNOWLEDGEMENTS

This research was supported by the National Science Foundation Grant Number DMI-9871185, the grant from the U.S. Air Force Research Laboratory contract # FA8650-04-C-5704, and UMR Intelligent Systems Center. Their support is greatly appreciated.

REFERENCES

1. Liou, F.W.; Landers, R.G.; Choi, J.; Agarwal, S.; Janardhan, V.; Balakrishnan, S.N.,(2001) "Research and Development of a Hybrid Rapid Manufacturing Process," Proceedings of the Twelfth Annual Solid Freeform Fabrication Symposium, Austin, TX, pp. 138, August 6-8, 2001.

2. Eiamsa-ard, K., Liou, F.W., Landers, R.G., and Choset, H., Toward automatic process planning of a multi-axis hybrid laser aided manufacturing system: skeleton-based offset edge generation, Proceedings of DETC'03, September 2 – 6, 2003, Chicago, IL.

3. Ruan, Jianzhong; Eiamsa-ard, Kunnayut; Zhang, Jun and Liou, F.W., "Automatic Process Planning of a Multi-Axis Hybrid Manufacturing System", Proceedings of DETC'02, September 29—October 2, 2002 Montreal, CANADA.

4. Zhang, J.; Ruan, J.; and Liou, F.W. "Process Planning for a Five-Axis Hybrid Rapid Manufacturing Process", Proceedings of the Eleventh Annual Solid Freeform Fabrication Symposium, Austin, TX, pp. 243., August 2000.

5. Hongcheng Wang, James A. Stori, "A metric-based approach to 2D tool-path optimization for high-speed machining", ASME IMECE2002-MED-33610.

6. Kao, J., and Prinz, F.B., "Optimal Motion Planning for Deposition in Layered Manufacturing", Proceedings of DETC'98, September 13 - 16, 1998, Atlanta, GA.

7. A. Zelinsky, R. A. Jarvis, J. C. Byrne and S. Yuta, "Planning Paths of Complete Coverage of an Unstructured Environment by a Mobile Robot", Proceedings of International conference on Advanced Robotics, 1993.

8. Choi, B.K., and Park, S.C., A pair-wise offset algorithm for 2D point sequence curve, Computer –Aided Design. 1999:31(12):735-745.

9. Choi, B.K., and Kim, B.H., Die-cavity pocketing via cutting simulation, Computer Aided Design 1997:29(12):837-846.

10. Held, M., Lukas, G., and Andor, L., Pocket machining based on contour parallel tool path generation by means of proximity maps, Computer Aided Design 1994:189-203.

11. Misra, D., Sundararajan, V., Wright, P. K., Zig-Zag Tool Path Generation for Sculptured Surface Finishing, Dimacs Series in Discrete Mathematics and Theoretical Computer Science, 2005, VOL 67, 265-280.

12. Kunnayut Eiamsa-ard, F.W.liou, Lan Ren, H. Choset, Spiral-like path planning without gap for material deposition processes, ASME 2006 International Design Engineering Technical Conferences & Computers and Information in Engineering Conference, September 10-13, 2006.

13. Frank Liou, Jianzhong Ruan, A Hybrid Metal Deposition and Removal System for Rapid Manufacturing, International conference -- 2002 April: San Antonio, Metal powder deposition for rapid manufacturing.

14. Dutta, Debasish; Prinz, Fritz B.; Rosen, David; Weiss, Lee, "Layered Manufacturing: Current Status and Future Trends", Journal of Computing and Information Science in Engineering, March, 2001, Vol. 1, pp.60-71.

15. Zhiyang Yao, Satyandra K. Gupta, Cutter path generation for 2.5D milling by combining multiple different cutter path patterns, International Journal of Production Research, June 2004, Vol. 42, No. 11, 2141-2161.

16. Jianzhong Ruan, Lan Ren, Todd E. Sparks, Frank Liou, 2-D deposition pattern and strategy study on rapid manufacturing, Proceedings of IDETC/CIE 2006, September 10-13, 2006, Philadelphia, Pennsylvania.

17. Lan Ren, Ajay Panackal Padathu, Jianzhong Ruan, Todd Sparks and Frank W. Liou, Three dimensional die repair using a hybrid manufacturing system, Proceedings of the Seventeenth Annual Solid Freeform Fabrication Symposium, Austin, TX, August 14-16, 2006.

18. Kunnayut Eiamsa-ard, Hari Janardanan Nair, Lan Ren, Jianzhong Ruan, Todd Sparks, and Frank W. Liou, "Part Repair using a Hybrid Manufacturing System", Proceedings of the Sixteenth Annual Solid Freeform Fabrication Symposium, Austin, TX, August 1-3, 2005.

19. Choset, Howie, Coverage of Known Spaces: The Boustrophedon Cellular Decomposition, Autonomous Robots 9, no. 3 (2000): 247-253.

20. Acar, Ercan U, Choset, Howie, Rizzi, Alfred A, Atkar, Prasad N, Hull, Douglas, Morse Decompositions for Coverage Tasks, The International Journal of Robotics Research 21, no. 4 (2002): 331-344.

Table 1. Comparison of the length of the deposition path generated by different patterns.

Path pattern	offsetting	zigzag
Path length	82.7082 units	93.9717 units
Efficiency	Higher	Lower
Deposition void	Highly possible	Almost Impossible

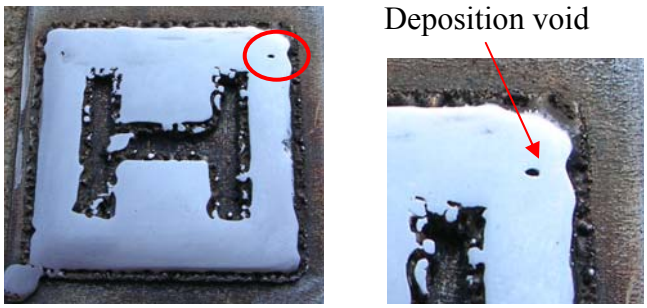

(a) (b)

Figure 1 Deposition void example a) deposit after machining out the top surface b) close up view.

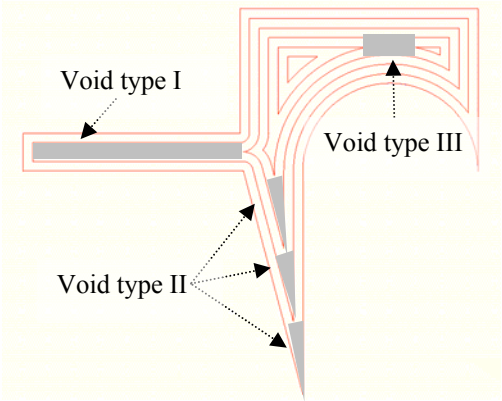

Figure 2 Different types of void often happened in deposition.

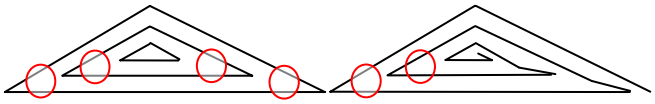

Figure 3 Deposition void occurrence using a) contour-parallel offsetting pattern and b) spiral offsetting pattern.

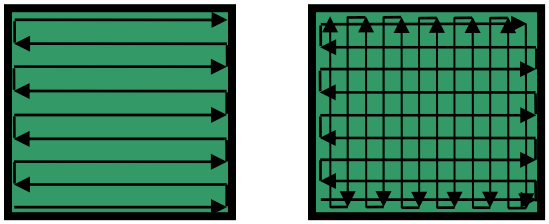

(a) (b)

Figure 4 Different zigzag toolpath generation patterns (a) Zigzag (fixed direction) (b) Zigzag (interlaced direction).

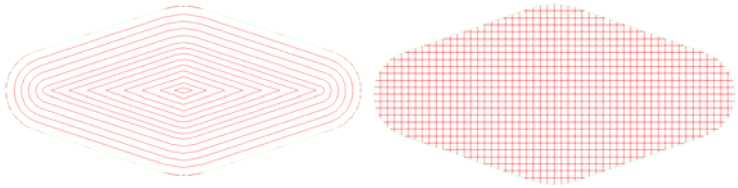

(a) (b)

Figure 5 Deposition toolpath generated by a) contour-parallel offsetting pattern b) adaptive zigzag pattern.

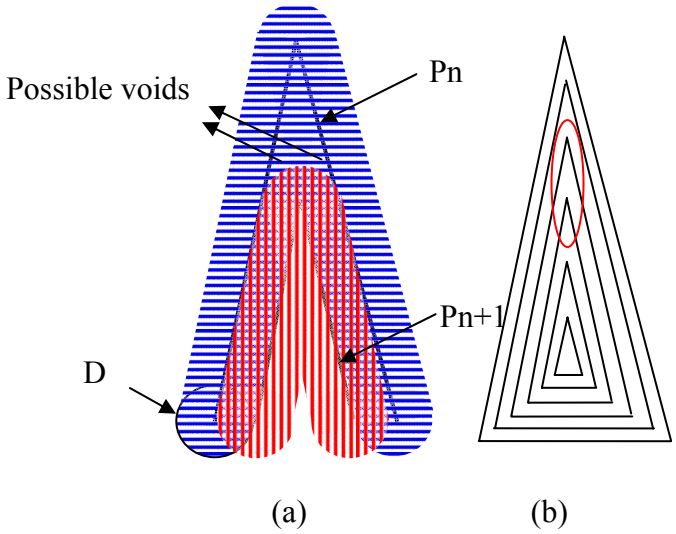

Figure 6 Principle of the occurrence of the deposition void.

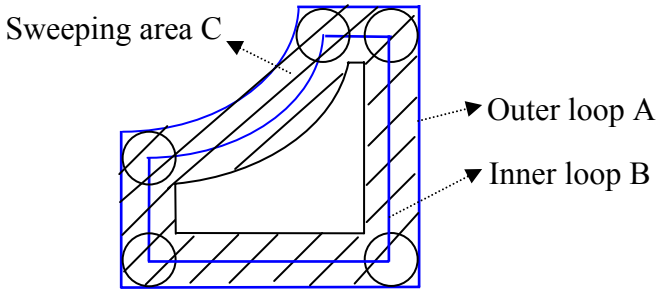

Figure 7 Prediction algorithm for deposition voids.

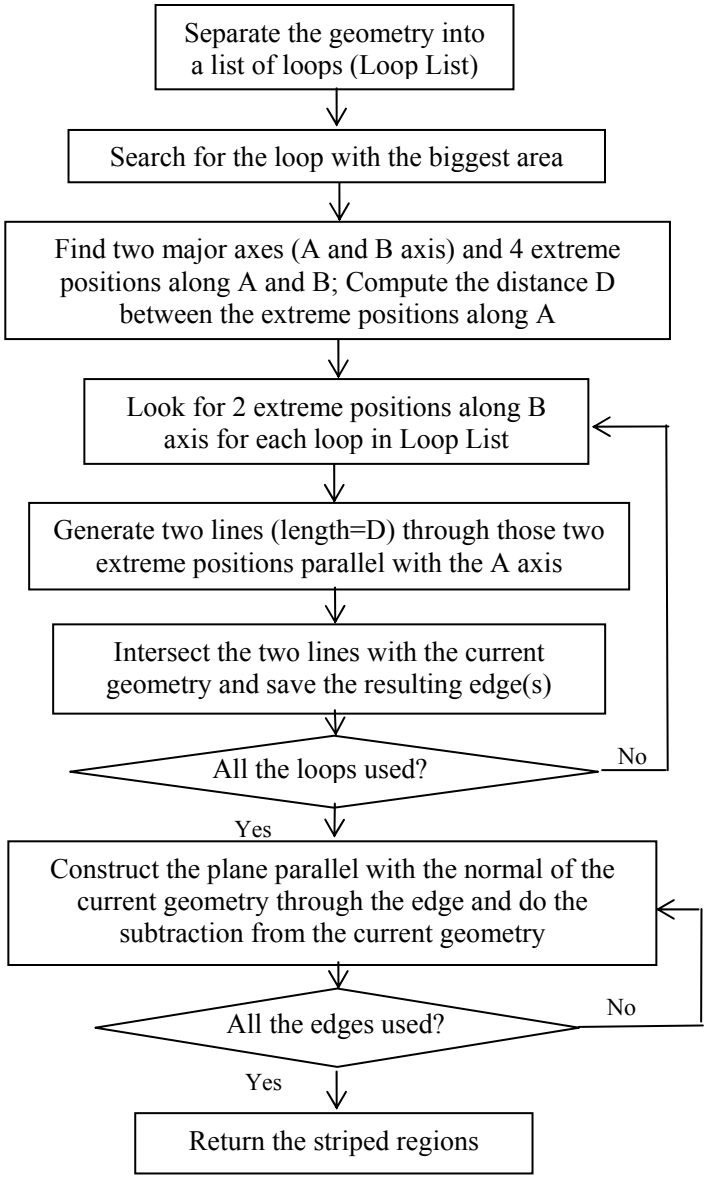

Figure 8 Flow chart of the cell decomposition algorithm.

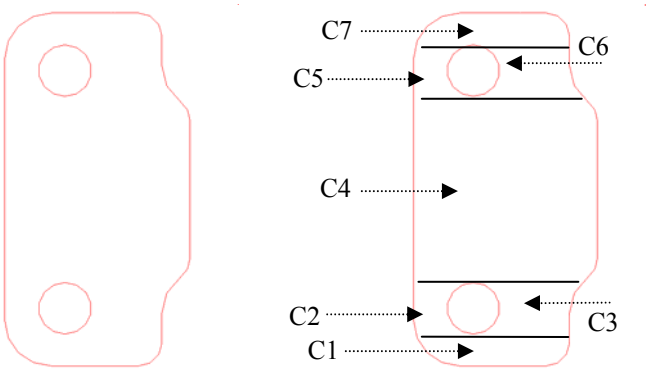

(a) Before decomposition (b) After decomposition

Figure 9 Example of 2D cell decomposition.

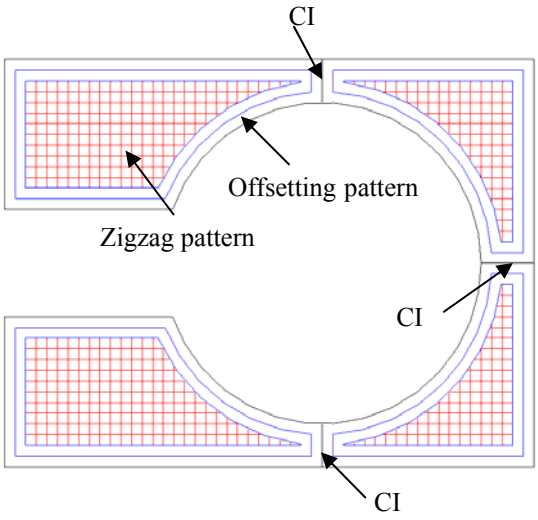

(a) Example I

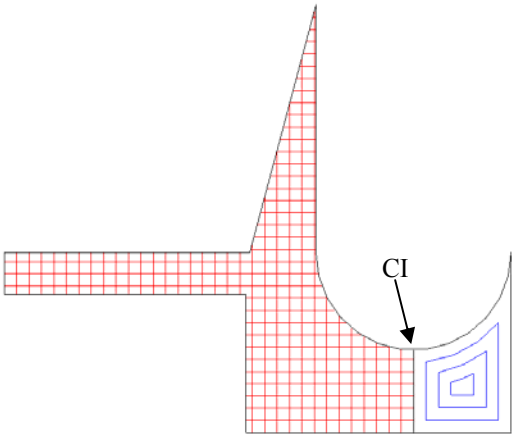

(b) Example II

Figure 10 Adaptive toolpath for complicated geometry.

Figure 11 Deposited part using the adaptive toolpath pattern after top surface machining.

PAPER III

PROCESS PLANNING STRATEGIES FOR SOLID FREEFORM FABRICATION OF METAL PARTS

Lan Ren, Todd Sparks, Jianzhong Ruan, Frank Liou

Department of Mechanical and Aerospace Engineering, University of Missouri-Rolla, Rolla, MO 65409

Abstract. Process planning of additive manufacturing of metals is a research interest because of the applications of solid freeform fabrication of metal parts in industry. The strategy is to transform the model of the part into the combinations of 2D layers which will be deposited using different fabrication methods. Process planning for metal deposition in this paper consists of three major modules: spatial decomposition, slicing of the part, and toolpath generation for every slicing layer. Algorithmic improvements are proposed and implemented for these major modules. For spatial decomposition, 3D part decomposition based on modular boundary models and centroidal axis extraction methods are combined to decompose parts more robustly and reliably. For generating slicing layers, a planning process for building non-uniform layers is investigated to greatly increase the variety of the parts which can be manufactured without the need of support structure. For toolpath generation methods, optimization of the generated toolpath is studied especially for complex thin-wall structure to ensure the deposition quality. Experiments were carried out to evaluate the improvements of the major modules of process planning strategies for rapid manufacturing.

Keywords: Solid Freeform Fabrication, Rapid Prototyping, Direct Metal Deposition, Process Planning, Spatial Decomposition, Centroidal Axis Extraction

Introduction. Rapid manufacturing technology has been applied to build functional parts in industry (Laeng 2000; Koch 2001; Dutta 2001; Liou 2002). The rapid prototyping process used in this paper is the Direct Metal Deposition (DMD) process, which utilizes a high power laser to melt metal powder layer by layer on the substrate to manufacture fully dense metal parts directly. This rapid manufacturing system is located in the Laser Aided Manufacturing Process (LAMP) lab at University of Missouri-Rolla.

Many process planning strategies and toolpath generation methods for rapid manufacturing are available in the literature (Ruan 2002; Kao 1999; Singh 2001; Zhang 2000; Pandey 2003; Kumar 2002; Eiamsa-ard 2003; Liou 2001). There are three major modules of process planning for the rapid manufacturing system in LAMP lab. They are spatial decomposition of CAD model of the part, adaptive slicing process of the decomposition results and toolpath generation for every slicing layer. For every module, different strategies and methods were investigated. As far as decomposition of complex parts is concerned, spatial decomposition (Ramaswami 1997) and the centroidal axis extraction method (Ruan 2005; Culver 2004; Sampl 2001) were advanced to decompose the part into several sub-components. For every sub-component, the building direction is consistent. Spatial decomposition is implemented by decomposing the part along the concave boundary silhouette edge of the part model. The disadvantage of spatial decomposition is that this method still cannot avoid the need of support structure which means that support structure is considered to assist in building complex parts. Centroidal

axis extraction method decomposes the part model by detecting the change of centroid of pre-sliced layers. For example, Figure 1 shows the CAD model of a part and the centroidal extraction results of the part model. As the figure shows, the part is decomposed into four components. Decomposition happens where certain amount of centroidal information change is detected. However, this implementation still has its own limitation. Illustrated in Figure 2, the centroidal axis of the shape does not indicate the change of the geometry and the deposition will fail without support structure. In this paper, centroidal axis extraction method and decomposition based on modular boundary models will be combined to increase the feasibility of decomposition process. The former method will be used as a default strategy, and the decomposition method will switch to the latter one if the centroidal positions are the same for the adjacent slicing layers but the rapid geometric change is detected by comparing the area of the adjacent slicing layers.

After decomposition of part model is finished, the slicing algorithm will be used to get the 2D slicing layers for every decomposed component. The slicing results will be uniform layers as shown in Figure 3(a). However, non-uniform layers as shown in Figure 3(b) will probably be generated using adaptive slicing procedure especially when slicing the parts which have curve features. The process planning strategy for building non-uniform layers will be another research issue covered in this paper. Every non-uniform layer will be considered as another part to build. The goal is to transform the non-uniform layer into a combination of uniform layers. The strategy for process planning of 3D non-uniform layers will be explained in the following sections in detail.

The final module is toolpath generation after the part model is decomposed and sliced into layers. Compared to the previous two modules, the coverage toolpath in rapid

prototyping has been studied more extensively as an important component of process planning (Ruan 2002; Zhang 2000; Eiamsa-ard 2003; Liou 2001). Although many researchers studied the optimization of the toolpath planning strategies (Wang 2002; Kao 1998; Zelinsky 1993), the major toolpath generation patterns in the current research work are still as follows: contour offsetting pattern (Choi 1999; Choi 1997; Held 1994) and zigzag pattern (Misra 2005). The contour offsetting pattern includes the contour-parallel offsetting pattern and spiral offsetting pattern (Kunnayut Eiamsa-ard 2006). The spiral offsetting pattern is the modified contour-parallel offsetting which has better connectivity between every connective offset loops. For the rapid manufacturing industry, the contour-parallel offsetting pattern and spiral offsetting pattern are often adopted due to the nature of additive manufacturing technology. In addition to the above patterns, in the research done by Yao and Gupta (Yao 2004), multiple cutter path patterns were combined for 2.5D milling to generate the improved cutter path. The objective of this strategy is to find the most efficient toolpath which is the shortest path to cover the area to be machined. And the computational time needed may be a bottleneck. In (Ruan 2006), combinations of the toolpath generation patterns have been studied in the deposition processes, and a deposition cell was defined. The deposition void was fixed by adjusting the toolpath, i.e., adding some straight lines to cover the area where a void may happen. This method can fill the small voids; however, some bigger voids cannot be filled with just several straight lines, and the surface flatness will be impaired as well. So, the method of filling the voids with several lines is not always effective. Another method is to decompose the target area into several loops and to use the different toolpath patterns in different loops. In (Ren 2007), an adaptive toolpath generation pattern was advanced where coverage and

efficiency are both considered as the objectives with the assumption that coverage has higher priority. The zigzag pattern (Ren 2006; Eiamsa-ard 2005) and contour-parallel offsetting pattern will be used as the candidates. The algorithm was developed to predict the possibility of the occurrence of deposition void and switch to the appropriate toolpath pattern automatically when needed.

This paper will focus on one kind of part which is complex thin-wall structure. In CAD modeling, a thin-wall structure is one kind of special body called shell body. Most toolpath planning is with regard to solid parts. Obviously, toolpath planning for thin-wall structure is different from other solid parts. As shown in Figure 4, it is a thin-wall structure with inner loop. The thickness shown as l in the Figure 4 is the major criteria to define a thin-wall structure. Depending on the operational parameters of the different rapid prototyping systems, the definition of the thin-wall structure is certainly different. In this paper, feature recognition of thin-wall structure is not the research focus. The user will decide whether the loaded part model is thin-wall structure or not. If a part includes some non-thin-wall features and some thin-wall features, it is also considered thin-wall structure here. Toolpath planning for complex thin-wall structure will also be demonstrated in following sections.

This paper is organized as follows: The decomposition method combining the centroidal axis extraction method and decomposition based on modular boundary models is illustrated in Section 2. The strategy for building 3D non-uniform layers is explained in Section 3. Toolpath planning for complex thin-wall structure is demonstrated in Section 4. The experiments are performed and the results are discussed in Section 5. The paper is concluded in Section 6. The entire algorithm in this paper was programmed using

HOOPS as the display engine and ACIS as the 3D modeling kernel and it has been developed using Visual C++ programming language. The CAD model in this paper is in .SAT format, which is the surface boundary representation of a solid model.

Adaptive Spatial Decomposition. Adaptive spatial decomposition was developed to enhance the performance of the centroidal axis extraction, method, especially when the centroidal information can not detect the change of the part geometry.

For example, Figure 5(a) is a part model of turbine blade. Figure 5(b) shows the centroidal information for every pre-sliced layer. It is clearly shown that the centroidal axis can not detect the geometry change because of the symmetric blades. The adaptive spatial decomposition strategy will be able to detect the failure of centroidal axis extraction and switch to the decomposition method based on modular boundary models. Boundary models are assumed to be modular boundary models, which are a class of part representations that describe a solid object as a set of face-abutting components or cells as shown in Figure 6. The cell interface is either concave edge or concave loop. If every point on an edge is concave, then this edge is concave edge. Loop consists of a list of edges in certain order and the loop is concave loop if every edge of this loop is concave edge. Figure 7(a) shows the cell interface which is concave edge and Figure 7(b) shows the cell interface which is concave loop. Adaptive spatial decomposition method can detect the geometry change by comparing every two connective pre-sliced layers when centroidal information remains the same. For example, Figure 8(a) and Figure 8(b) demonstrate the n^{th} and $n+1^{th}$ layer of pre-sliced layers. Subtraction result of these two layers is shown in Figure 8(c). Hence, the geometry change can be detected by comparing

the area of two connective layers. Decomposition method will switch once the centroidal positions are the same for the adjacent slicing layers but the rapid geometric change is detected by comparing the area of the adjacent slicing layers.

The algorithm of decomposition based on modular boundary models is shown in the flowchart in Figure 9. The turbine blade will still be used as an example to explain the flowchart of this decomposition algorithm. The first major step is to find all the concave loops in the body which are highlighted in Figure 10. All the loops will be saved in a list. Every loop will be used later to decompose the body. In this case, three concave loops are found. Then, the 2D projection plane is obtained for every concave interaction loop CIL and the centroid C and normal vectors, v and -v, for the projection plane are calculated as shown in Figure 11. Based on the normal vector, the two extreme positions P1 and P2 on the concave loop along the normal vector v and –v are calculated using equation (1) and (2). The next step is to decompose the part by constructing appropriate slicing plane which is subroutine A as demonstrated in Figure 9. The following steps are conducted to decompose the part by constructing appropriate slicing planes.

1. Construct two planes S1, S2 using P1, v and P2, -v, respectively.
2. Slice current body using S1 to get a list of surfaces.
3. Find surface F1 closest to centroid C in the list.
4. Slice current body using S2 to get a list of surfaces.
5. Find surface F2 closest to centroid C in the list.
6. Choose smaller one between F1 and F2 and save as F.
7. Subtract from current body using surface F and get two decomposed bodies.
8. Save current body and two decomposed bodies in the final list.

9. Output two decomposed bodies.

$$\overrightarrow{EP_v}^{+} = \vec{C} + [[(\overrightarrow{P_1} - \vec{C}) \bullet \bar{v}] + \varepsilon] \bullet \bar{v} \quad (1)$$

$$\overrightarrow{EP_v}^{-} = \vec{C} + [[(\overrightarrow{P_2} - \vec{C}) \bullet (-\bar{v})] + \varepsilon] \bullet (-\bar{v}) \quad (2)$$

Construction of the slicing planes needs the extreme points to determine the positions of slicing planes shown in the following equation (1) and (2). A pair of slicing planes, S1 and S2, is constructed through position EPv+ and EPv- using the normal vector v and –v. Two surfaces, F1 and F2, can be generated by slicing the body with the pair of slicing planes, S1 and S2 as shown in Figure 12. The smaller face between F1 and F2 is selected as the final surface F. In this case, F2 is selected as the final surface F because it is the smaller one. Finally, F is applied to decompose the turbine blade into two sub-components. These two sub-components will be marked as “to-be-decomposed” in case more decomposition is needed and the current body, which is the entire turbine blade, will be marked as “decomposed”. Both the current body and those two decomposed sub-components need to be saved in the final list. Every concave loop in the list will be used once to decompose all the “to-be-decomposed” body in the final list. The decomposition will end until every concave loop is used. The final decomposed components include all the “to-be-decomposed” body in the final list. Figure 13 illustrated the decomposition results of the turbine blades. Hence, decomposition based on modular boundary models can decompose those parts which can not be decomposed using centroidal axis extraction method. The adaptive spatial decomposition combines both two methods as candidate. It also involves the detection of the geometry change when the centroidal information keeps the same. Centroidal axis extraction method is the

default choice and it will switch to decomposition method based on modular boundary models when geometry change is detected but centroidal information fails to detect the change.

Manufacturing of Non-uniform Layers. Non-uniform layer occurs when slicing a part which has curve features. For example, Figure 14 shows an arch. After adaptive slicing, every slicing layer will be a non-uniform layer, called a "unit layer" in this paper. Every non-uniform layer will be considered a normal part which is sliced using parallel planes. That means every non-uniform layer is composed of uniform layers. Figure 15 shows the non-uniform layer sliced into uniform layers. After the uniform slicing layers of the non-uniform layer are obtained, the toolpath will be generated for every uniform slicing layer to build the non-uniform unit layer, as shown in Figure 16.

It is worth noting that the determination of the thickness of unit layer is critical to build the parts which have 3D non-uniform layer generated using adaptive slicing. Time efficiency will be decreased if the unit layer is too thin. The unit layer can not be too thick either; otherwise, the deposit probably will not be enough to ensure the curve feature after surface finish machining. Figure 17 demonstrates the steps about how to figure out the angle r when slicing an arch-shape part so that s is larger than the actual track width of the deposition process. In the equations, "*D*" represents the laser spot size. "*O*" represents overlap between every connective tracks. "*d*" denotes the actual track width during depositing process with overlap factor being considered. "*s*" denotes the difference along the radial direction of the unit layer. "t" denotes the radius of the curve feature of the part.

$$d = D(1-O) \tag{3}$$

$$s = t - t * \cos(r) \tag{4}$$

$$s \le d \tag{5}$$

$$r \le \cos^{-1}\left(\frac{t - D(1-O)}{t}\right) \tag{6}$$

The above equations give the maximum value of angle r for depositing a 3D unit layer using rapid manufacturing method mentioned above in this paper. After the unit layer is obtained, the unit layer will be considered to be a new part to be sliced using the specified layer thickness according to the different rapid prototyping systems. Hence, the non-uniform layer can be built using combination of uniform layers by choosing the appropriate thickness of the unit layer based on the specified operational parameters of different rapid manufacturing systems.

Optimization of Toolpath Generation for Thin-wall Structure. The thickness of the part has to be at least larger than 2*d so that at least one contour-parallel offset loop can be obtained. So, it will be considered to be thin-wall structure in this paper if the thickness is smaller than 2*d or the part has at least one feature whose thickness is smaller than 2*d. Thin-wall structure parts are divided into two groups: thin-wall parts with inner loops and thin-wall parts without inner loops. Different strategies are investigated for different categories of thin-wall structures. For example, Figure 18 shows the thin-wall part without inner loops. Also the part has thin-wall features in stead of complete thin-wall structure. For this kind of thin-wall parts, contour-parallel offsetting toolpath generation pattern is used to obtain the initial toolpath. However, the initial toolpath need to be modified. The strategy is to add an extra toolpath if the first loop has less edges than the outer loop which is the profile of the whole part as shown in Figure

18(b). The detailed algorithm realization is shown in Figure 18 (c). It can be clearly observed that the first offset loop has one less edge compared with the outer loop because of the thin-wall feature. i.e., the disappeared edge can be considered as a point on the first loop after disappearing. Here, the middle point of the edge is used to generate an extra toolpath as shown in Figure 18 (b).

For thin-wall structure with inner loops, no extra toolpath needs to be added. However, the toolpath needs to be reorganized to ensure deposition quality. Because of the existence of inner loops, the generated contour-parallel offsetting path is broken into segments. It is important to organize these toolpath into an array. The goal is to finish deposition quickly and the deposition quality must be guaranteed at the same time. For every slicing layer, the deposition toolpath includes three parts. First, a periphery loop needs to be found for the layer. Next, all the inner loops for the layer need to be traveled after the periphery loop is traveled. Finally, the majority of the toolpath is generated using the contour-parallel offsetting toolpath pattern. There are still two categories of deposition path in this case. One is the category of those paths along which some materials need to be deposited in order to build the part. The other is the category of those paths along with none of materials should be deposited in order to ensure the deposition quality. This latter kind of toolpath is called transition toolpath.

The flowchart in Figure 19 demonstrates the toolpath generation process for this kind of complex thin-wall structure in detail. Figure 20 is used to help explaining the flowchart. Figure 20(a) is the layer to be deposited and Figure 20(b) is the deposition toolpath generated. The red toolpath is the toolpath along which materials need to be deposited. The connective lines in black are the transition toolpath. The laser and powder

feeder should be turned off when traveling along the transition toolpath. That means the deposition should stop when traveling along the transition path. After the toolpath is generated, the transition path will be obtained by connecting two inconsecutive offsetting edges with straight lines.

It can be clearly seen that the geometry in Figure 20 has one periphery loop and three inner loops. As demonstrated in the flowchart, the periphery loop needs to be saved in the final path list first of all. Then the other three inner loops need to be saved in the final path list and they are located after the periphery loop. Then all the offsetting loops need to be reorganized before saving into the final path list. As Figure 20(b) shows, two of the offsetting loops are divided into broken edges at points A, B, C, D, E, F, G and H by the inner loops. At those points, straight lines are added to connect all the inconsecutive edges in one loop. Those connecting lines need to be marked as transition path. The laser and powder feeder must be turned off when traveling along those transition paths.

Examples and Discussions. Some experiments of part building have been carried out to evaluate the improved process planning for the hybrid manufacturing system. In the following experiment, the Nuvonyx direct diode laser was used and the laser processing parameters for cladding steel H13 powder were 600W with a stand off distance from the nozzle to the top of the clad of 0.5 inch. The travel speed was 20 inches per minute. The powder feed rate for H13 powder was 8 gram per minute. The track width used here is 0.1 inch with the overlap being 50%. Figure 21 is the complex thin-

wall part built by the optimized toolpath mentioned above. As the Figure shows, this part includes thin-wall features.

Conclusions. This paper focuses on the improvement on major modules of process planning framework for rapid manufacturing of metal parts. In this paper, (i) Adaptive spatial decomposition method is advanced to combine the advantage of the centroidal axis extraction method and decomposition method based on modular boundary models. It can compensate for the failure of the centroidal axis extraction method when the centroidal information can not detect the geometry change; (ii) The strategy for building non-uniform layers is investigated. Non-uniform unit layers are sliced into uniform layers so that non-uniform layers can be built by depositing the combination of a series of uniform layers; (iii) toolpath generation for complex thin-wall structure is studied as well. The optimization and reorganization algorithms are advanced to ensure the deposition quality of the complex thin-wall structure. By the experimental validations, it is proven that the above improvements can help to build the functional metal parts more efficiently and reliably.

Acknowledgements. This research was supported by the National Science Foundation grants DMI-9871185 and IIP-0637796, the grant from the U.S. Air Force Research Laboratory contract # FA8650-04-C-5704. The support from Boeing Phantom Works, Product Innovation and Engineering, LLC, Spartan Light Metal Products Inc, UMR Intelligent Systems Center, and UMR Manufacturing Engineering Program, is also greatly appreciated.

References.

1. Choi, B.K., and Park, S.C., A pair-wise offset algorithm for 2D point sequence curve, Computer –Aided Design. 1999:31(12):735-745.

2. Choi, B.K., and Kim, B.H., Die-cavity pocketing via cutting simulation, Computer Aided Design 1997:29(12):837-846.

3. Corney, Jonathan, Lim, Theodore, "3D Modeling with ACIS," 2001.

4. Culver, Tim; Keyser, John, Manocha, Dinesh, "Exact computation of the medial axis of a polyhedron," Computer Aided Geometric Design, 21, 2004, pp.65-98.

5. Dutta, Debasish, Prinz, Fritz B., Rosen, David, and Weiss, Lee, "Layered Manufacturing: Current Status and Future Trends," Journal of Computing and Information Science in Engineering, March, 2001, Vol. 1, pp.60-71.

6. Eiamsa-ard, K., Liou, F.W., Landers, R.G., and Choset, H., "Toward automatic process planning of a multi-axis hybrid laser aided manufacturing system: skeleton-based offset edge generation," Proceedings of DETC'03, September 2 – 6, 2003, Chicago, IL.

7. Eiamsa-ard, Kunnayut liou, F. W., Ren, Lan, Choset, H., "Spiral-like path planning without gap for material deposition processes," ASME 2006 International Design Engineering Technical Conferences & Computers and Information in Engineering Conference, September 10-13, 2006.

8. Eiamsa-ard, Kunnayut, Hari Janardanan Nair, Ren, Lan, Ruan, Jianzhong, Sparks, Todd, and Liou, Frank W., "Part Repair using a Hybrid Manufacturing System", Proceedings of the Sixteenth Annual Solid Freeform Fabrication Symposium, Austin, TX, August 1-3, 2005.

9. Held, M., Lukas, G., and Andor, L., Pocket machining based on contour parallel tool path generation by means of proximity maps, Computer Aided Design 1994:189-203.

10. Kao, J., Process planning for additive/subtractive solid freeform fabrication using medial axis transform, Ph. D. Thesis, Stanford University, CA.

11. Kao, J., and Prinz, F.B., "Optimal Motion Planning for Deposition in Layered Manufacturing", Proceedings of DETC'98, September 13 - 16, 1998, Atlanta, GA.

12. Koch, J.L & Mazumder , J.M(2001), "Rapid Prototyping by Laser Cladding," International journal of powder metallurgy. 37(2): 31.

13. Kumar, Madhup and Choudhury, A. Roy, "Adaptive slicing with cubic path approximation," Rapid Prototyping, Vol. 8. No. 4, 2002, pp. 224-232.

14. Laeng, J., Stewart, J. G., and Liou, F. W., (2000) "Laser Metal Forming Processes For Rapid Prototyping – A Review," International Journal of Production Research, Vol 38, No.16, 3973-3996, 2000.

15. Liou, Frank, Ruan, Jianzhong, "A Hybrid Metal Deposition and Removal System for Rapid Manufacturing," International conference -- 2002 April: San Antonio, Metal powder deposition for rapid manufacturing.

16. Liou, Frank. W., Choi, J., Landers, R. G., V. Janardhan, S. N. Balakrishnan, S. Agarwal, "Research and Development of a Hybrid Rapid Manufacturing process," Solid Freeform Fabrication Symposium, Austin, TX, 2001.

17. Misra, D., Sundararajan, V., Wright, P. K., "Zig-Zag Tool Path Generation for Sculptured Surface Finishing," Dimacs Series in Discrete Mathematics and Theoretical Computer Science, 2005, VOL 67, 265-280.

18. Pandey, Pulak Mohan; Reddy, N. Venkata and Dhande, Sanjay G., "Slicing procedures in layered manufacturing: a review," Rapid Prototyping Journal, Vol. 9, No. 5, 2003, pp.274-288.

19. Ramaswami, Krishnan, Yamaguchi, Yasushi, fritz B. Prinz, Spatial partitioning of solids for solid freeform fabrication, Proceedings of the fourth ACM symposium on Solid modeling and applications, Atlanta, Georgia 1997.

20. Ren, Lan, Ruan, Jianzhong, Kunnayut Eiamsa-ard, Liou, Frank, "Adaptive Deposition Coverage Toolpath Planning for Metal Depositon Process," Proceedings of DETC 2007, September 4-7, 2007, Las Vegas, Nevada.

21. Ren, Lan, Ajay Panackal Padathu, Ruan, Jianzhong, Sparks, Todd and Liou, Frank W., "Three dimensional die repair using a hybrid manufacturing system," Proceedings of the Seventeenth Annual Solid Freeform Fabrication Symposium, Austin, TX, August 14-16, 2006.

22. Ruan, Jianzhong, Ren, Lan, Sparks, Todd E., Liou, Frank, "2-D deposition pattern and strategy study on rapid manufacturing," Proceedings of IDETC/CIE 2006, September 10-13, 2006, Philadelphia, Pennsylvania.

23. Ruan, Jianzhong; Eiamsa-ard, Kunnayut; Zhang, Jun and Liou, F.W., "Automatic Process Planning of A Multi-Axis Hybrid Manufacturing System," Proceedings of DETC'02, September 29—October 2, 2002 Montreal, CANADA.

24. Ruan, Jianzhong, Eiamsa-ard, Kunnayut, Liou, Frank. W., "Automatic Multi-axis Slicing Based on Centroidal Axis Computation," Proceedings of DETC'05, September 24-28, 2005, Long Beach, CA.

25. Sampl, P., “Medial Axis Construction in Three Dimensions and its Application to Mesh Generation,” Engineering with Computers, 2001, 17, pp.234-248.

26. Singh, Prabhjot; Dutta, Debasish, “Multi-Direction Slicing for Layered Manufacturing”, Journal of Computing and Information Science in Engineering, June, 2001, Vol. 1, pp.129-142.

27. Wang, Hongcheng, Stori, James. A., “A metric-based approach to 2D tool-path optimization for high-speed machining”, ASME IMECE2002-MED-33610.

28. Yao, Zhiyang, Gupta, Satyandra K. Cutter, “path generation for 2.5D milling by combining multiple different cutter path patterns,” International Journal of Production Research, June 2004, Vol. 42, No. 11, 2141-2161.

29. Zelinsky, A., Jarvis, R. A., Byrne, J. C., Yuta, S., “Planning Paths of Complete Coverage of an Unstructured Environment by a Mobile Robot”, Proceedings of International conference on Advanced Robotics, 1993.

30. Zhang, Jun.; Ruan, Jianzhong; and Liou, Frank. W. “Process Planning for a Five-Axis Hybrid Rapid Manufacturing Process,” Proceedings of the Eleventh Annual Solid Freeform Fabrication Symposium, Austin, TX, pp. 243., August 2000.

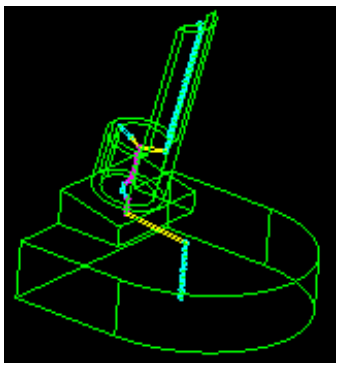

(a) 3D part model

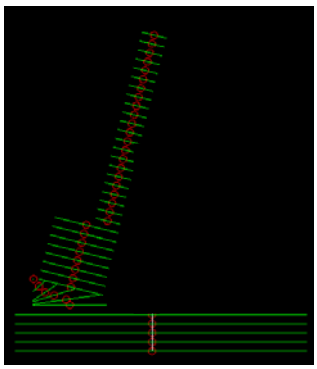

(b) Extracted centroidal information

Figure 1 Centroidal extraction of CAD model.

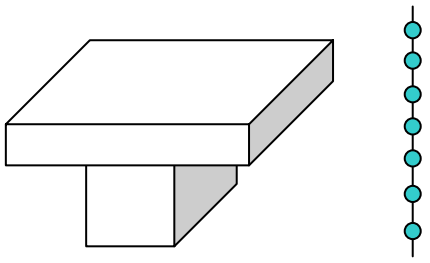

Figure 2 Centroidal axis fails to detect the geometric change.

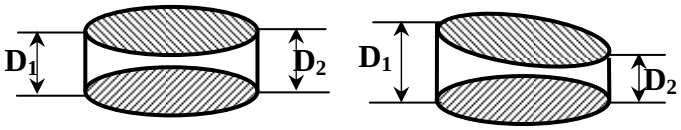

(a) Uniform layer $D_1 = D_2$ (b) Non-uniform layer $D_1 \neq D_2$

Figure 3 Uniform and Non-uniform Layers.

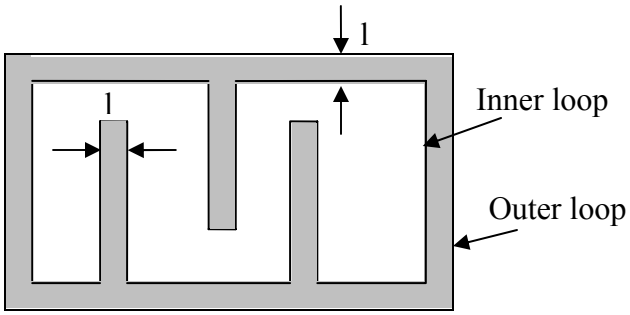

Figure 4 Thin-wall structures with inner loop.

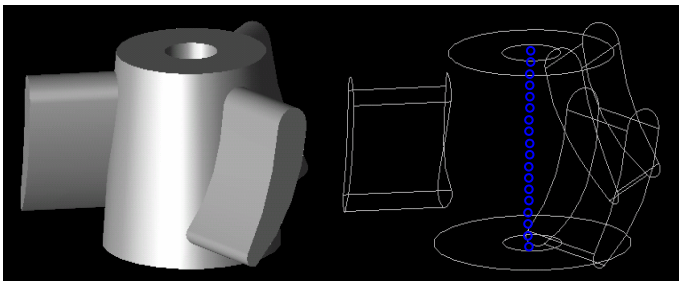

(a) (b)

Figure 5 (a) part model of turbine blade (b) centroidal information for the part model using centroidal axis extraction.

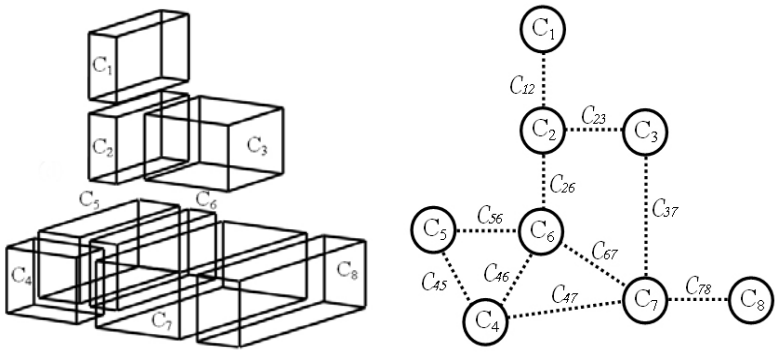

Figure 6 CELL-adjacency graph of non-manifold body (Corney 2001).

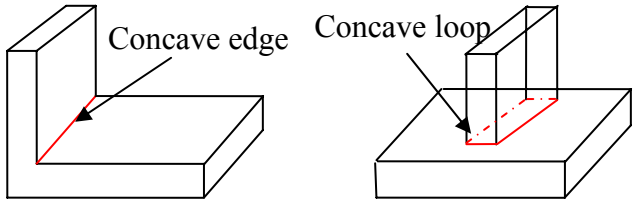

Figure 7 Cell interface (a) concave edge (b) concave loop.

(a) n^{th} layer b) $n+1^{th}$layer (c) area of $n+1^{th}$-n^{th}

Figure 8 Detection of geometry change when centroidal axis remains the same.

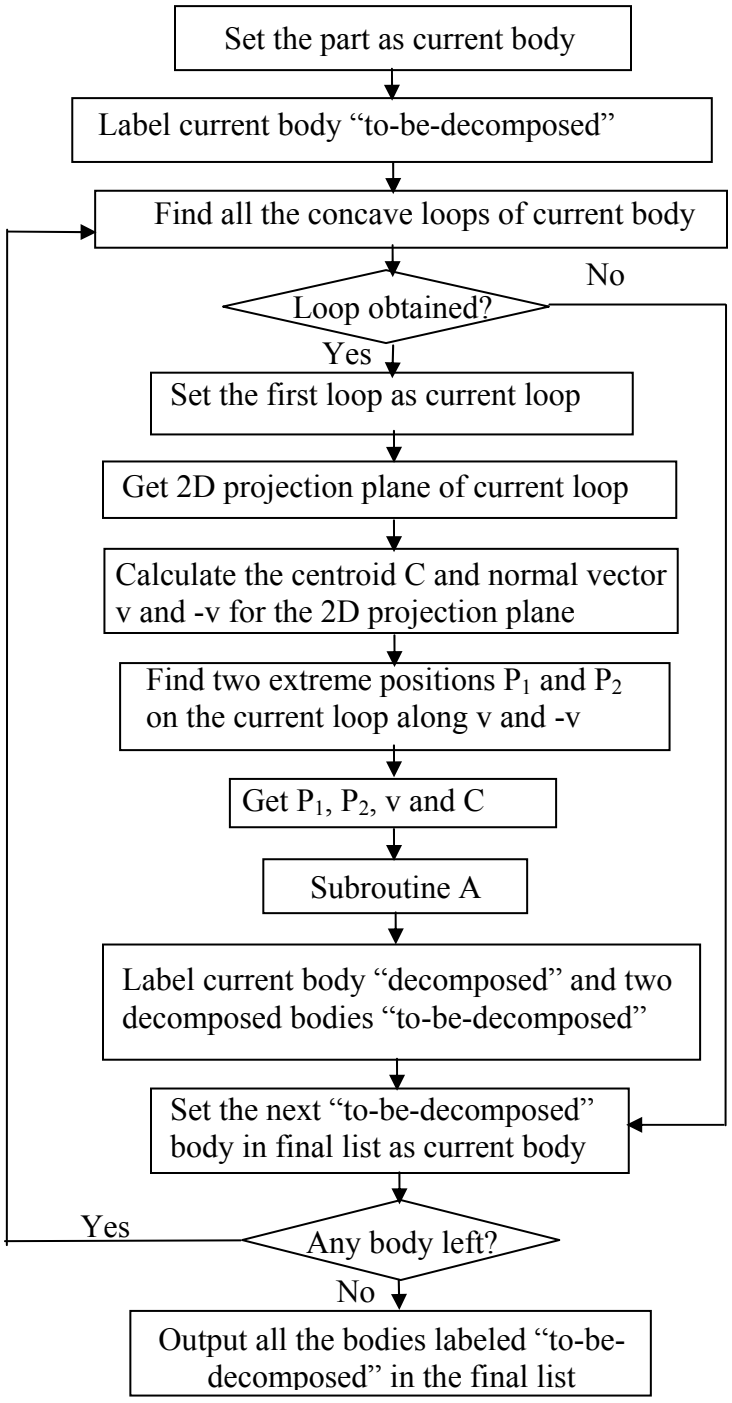

Figure 9 Flowchart of decomposition method based on modular boundary.

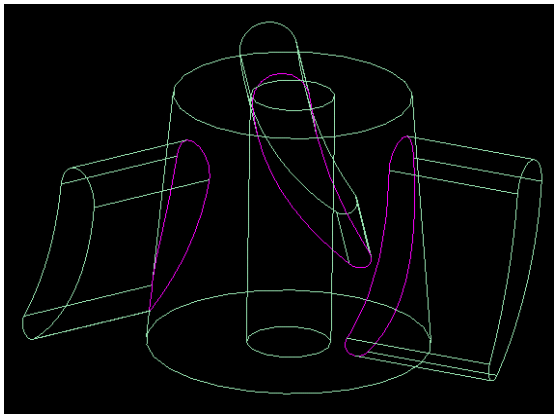

Figure 10 Concave loops found in the body.

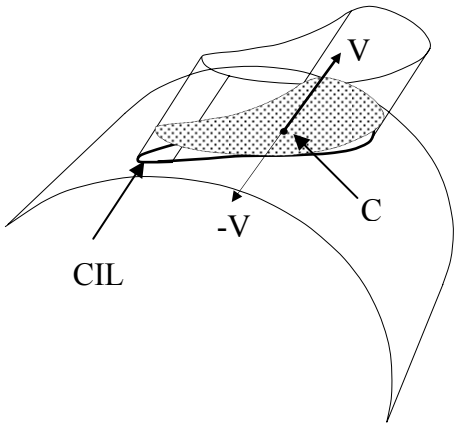

Figure 11 Projection plane of concave loop.

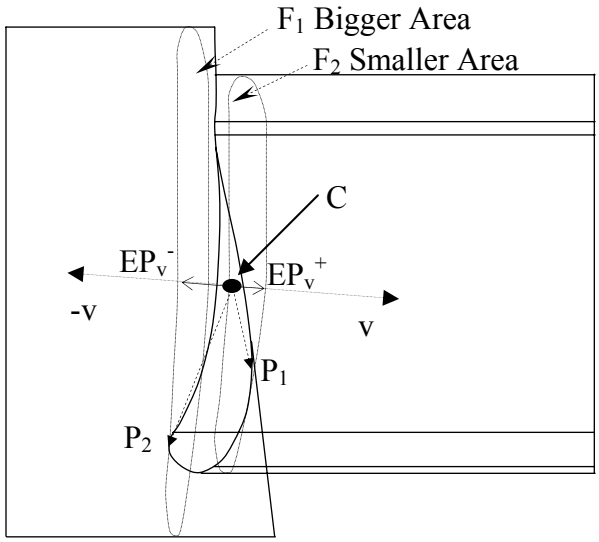

Figure 12 Calculation of decomposing planes.

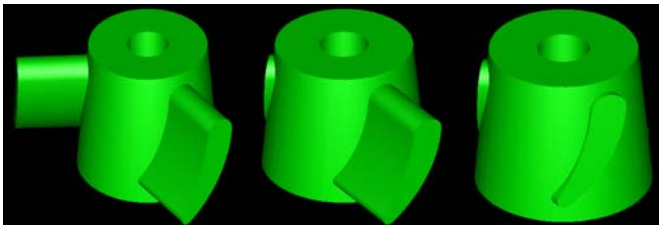

Figure 13 Turbine blades after decomposition.

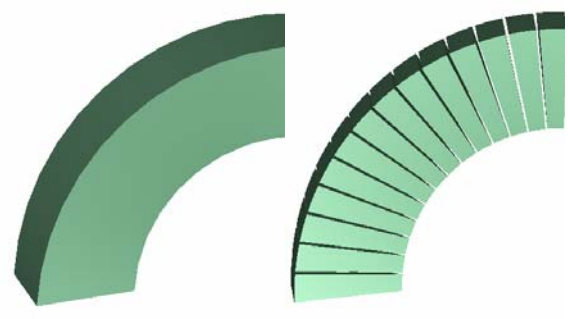

Figure 14 Part which has non-uniform layers after slicing.

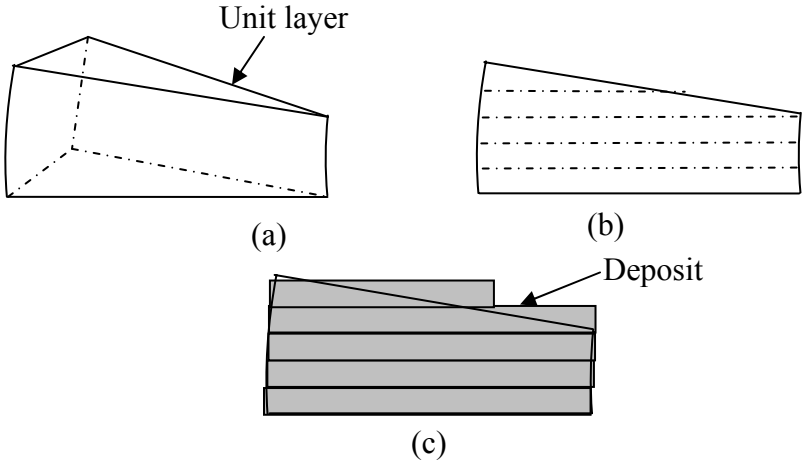

Figure 15 Slicing results of a unit layer (a) one unit layer (b) slicing results (c) unit layer after deposition.

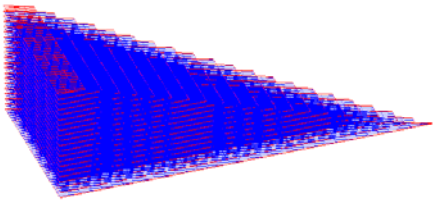

Figure 16 Toolpath for single non-uniform layer (Isotropic view).

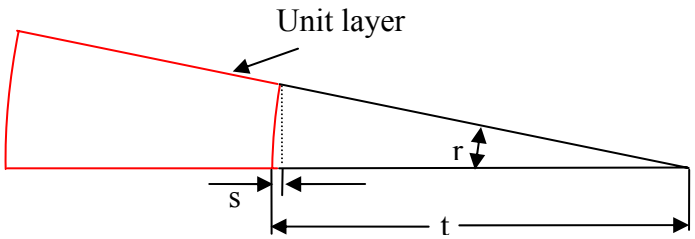

Figure 17 Calculation of the thickness of the unit layer.

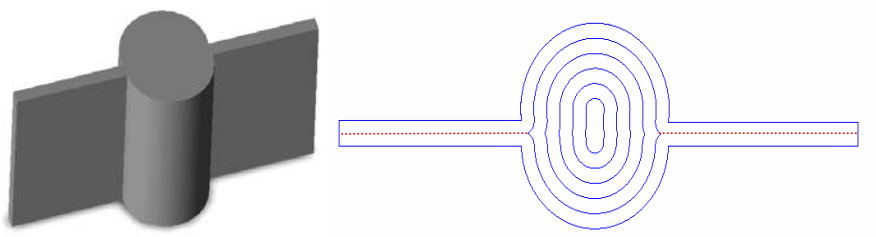

(a) thin-wall part (b) modified toolpath

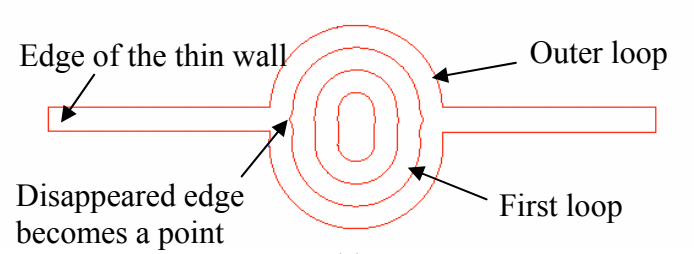

(c)

Figure 18 Thin-wall structures without inner loop.

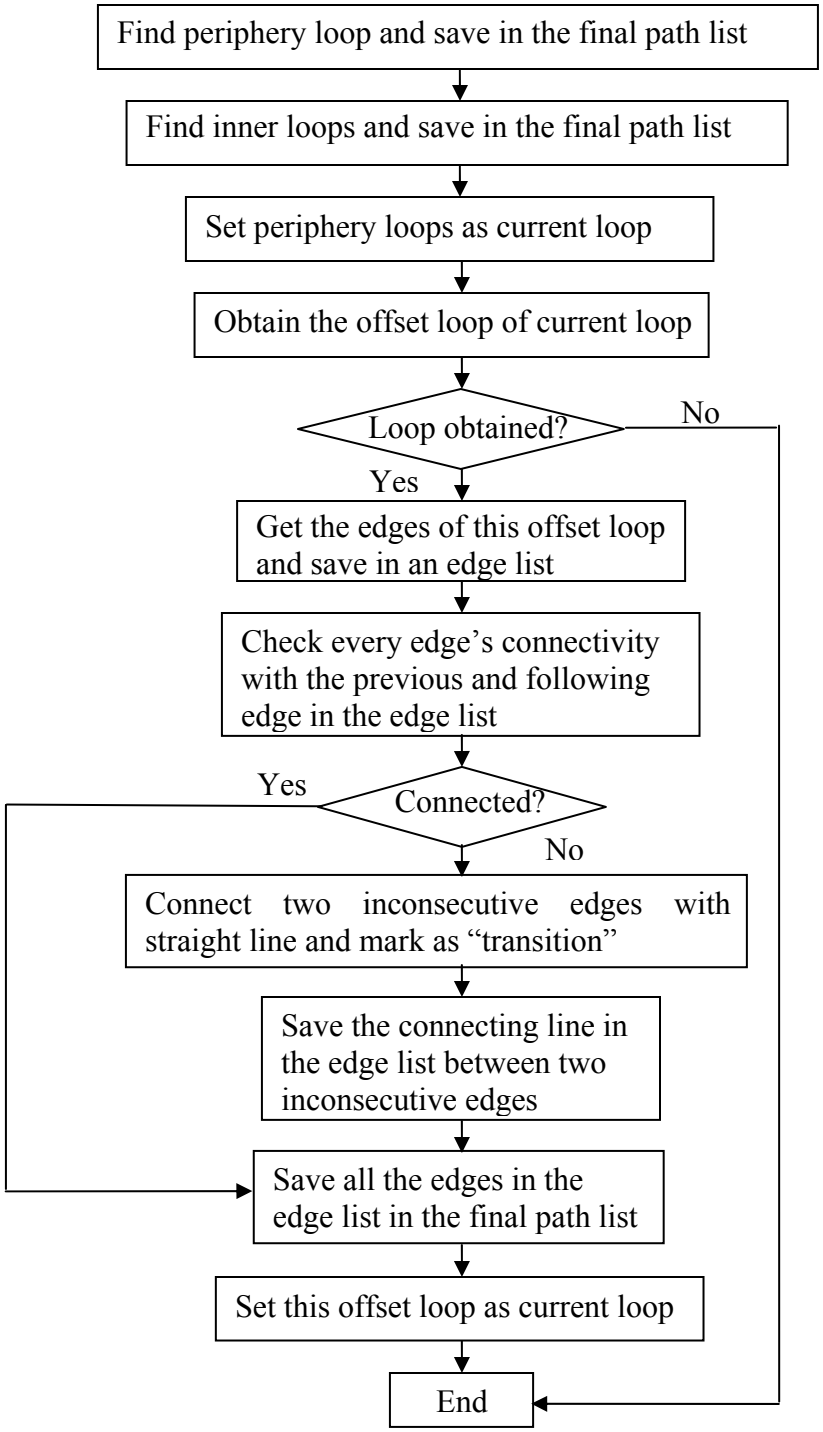

Figure 19 Flowchart of the optimization of offsetting toolpath for thin-wall structure.

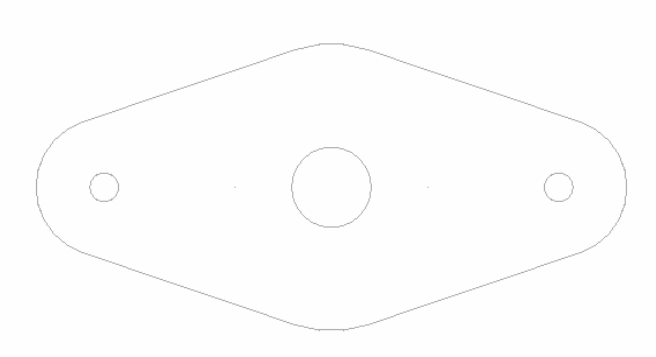

(a) Geometry of slicing layer

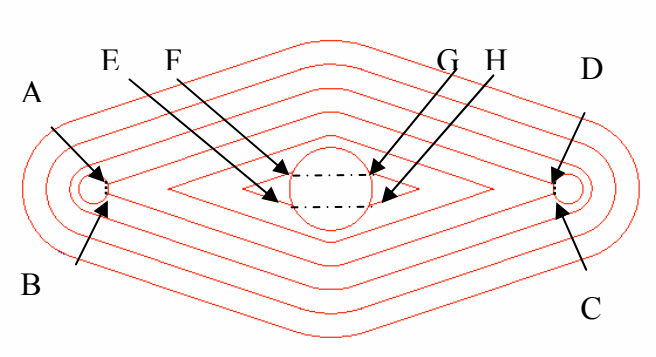

(b) Contour-parallel toolpath generated

Figure 20 To-be-organized contour-parallel offsetting toolpath.

(a) Solid CAD model of the thin-wall part (b) Generated offsetting toolpath

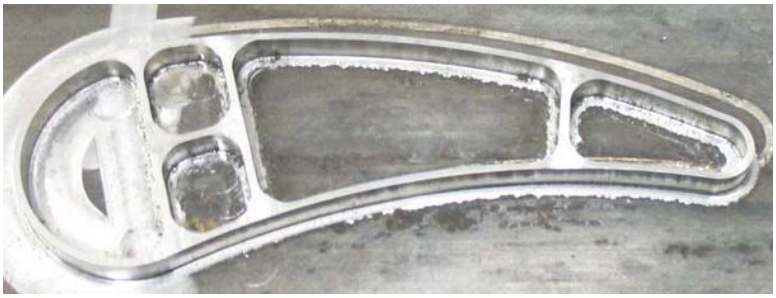

(c) Thin-wall deposit

Figure 21 Thin-wall part using deposition.

VITA

Lan Ren was born on June 26, 1979 in Hefei County, Anhui province, P. R. China. Her pre-college education was taken in Hefei county, Anhui province, P. R. China. She attended Hefei University of Technology where she received her B.S. and M.S. in Mechanical Engineering in 2001 and 2004, respectively.

Since August 2004, she joined Dr. Frank Liou's group for her PhD program in Mechanical Engineering at University of Missouri-Rolla, Rolla, MO, USA. She has held a Graduate Research Assistantship and Graduate Teaching Assistantship during her study at University of Missouri-Rolla. In May 2008, she received her PhD in Mechanical Engineering from University of Missouri-Rolla.